Coccolithophore growth and calcification in a changing ocean

Kristen M. Krumhardt[a], Nicole S. Lovenduski[b], M. Debora Iglesias-Rodriguez[c], Joan A. Kleypas[d]

[a]Environmental Studies Program and Institute of Arctic and Alpine Research, University of Colorado Boulder, Boulder, Colorado, U.S.A.
[b]Department of Atmospheric and Oceanic Sciences and Institute of Arctic and Alpine Research, University of Colorado Boulder, Boulder, Colorado, U.S.A.
[c]Department of Ecology, Evolution, and Marine Biology, and Marine Science Institute, University of California Santa Barbara, Santa Barbara, California, U.S.A.
[d]Climate and Global Dynamics, National Center for Atmospheric Research, Boulder, Colorado, U.S.A.

Abstract

Coccolithophores are the most abundant calcifying phytoplankton in the ocean. These tiny primary producers have an important role in the global carbon cycle, substantially contributing to global ocean calcification, ballasting organic matter to the deep sea, forming part of the marine food web base, and influencing ocean-atmosphere CO_2 exchange. Despite these important impacts, coccolithophores are not explicitly simulated in most marine ecosystem models and, therefore, their impacts on carbon cycling are not represented in most Earth system models. Here, we compile field and laboratory data to synthesize overarching, across-species relationships between environmental conditions and coccolithophore growth rates and relative calcification (reported as a ratio of particulate inorganic carbon to particulate organic carbon in coccolithophore biomass, PIC/POC). We apply our relationships in a generalized coccolithophore model, estimating current surface ocean coccolithophore growth rates and relative calcification, and projecting how these may change over the 21st century using output from the Community Earth System Model large ensemble. We find that average increases in sea surface temperature of ~2-3°C leads to faster coccol-

---

*Kristen M. Krumhardt
Email address: `kristen.krumhardt@colorado.edu` (Kristen M. Krumhardt)

ithophore growth rates globally ($>10\%$ increase) and increased calcification at high latitudes. Roughly an ubiquitous doubling of surface ocean pCO_2 by the end of the century has the potential to moderately stimulate coccolithophore growth rates, but leads to reduced calcification ($\sim25\%$ decrease). Decreasing nutrient availability (from warming-induced increases in stratification) produces increases in relative calcification, but leads to $\sim25\%$ slower growth rates. With all drivers combined, we observe decreases in calcification and growth in most low and mid latitude regions, with possible increases in both of these responses in most high latitude regions. Major limitations of our coccolithophore model stem from a lack of conclusive physiological responses to changes in irradiance (we do not include light limitation in our model), and a lack of physiological data for major coccolithophore species. Species within the *Umbellosphaera* genus, for example, are dominant in mid to low latitude regions where we predict some of the largest decreases in coccolithophore growth rate and calcification.

1. Introduction

Coccolithophores are a significant component of the phytoplankton community, comprising up to 20% of the phytoplankton carbon pool in open ocean regions (Poulton et al., 2007) and forming prolific blooms at higher latitudes
5 (Iglesias-Rodríguez et al., 2002; Balch et al., 2007). Not only do coccolithophores form part of the marine food web base, they also have a unique influence on the global carbon cycle. Performing both photosynthesis and calcification, coccolithophores influence ocean-atmosphere CO_2 exchange and the export of organic and inorganic carbon to the deep ocean through the ballasting effects of their
10 calcium carbonate shells and subsequent sedimentation to the deep sea (Klaas and Archer, 2002). The growth and calcification of coccolithophores, however, could be impacted by impending alterations to the oceanic environment from anthropogenic climate change.

As CO_2 concentrations in the atmosphere continue to rise from anthro-
pogenic emissions, we expect three major changes in the surface ocean. First,
surface waters will warm as the ocean absorbs excess heat from the atmosphere.
Second, this warming will increase stratification in the upper ocean, decreas-
ing nutrient availability for organisms living in the upper photic zone (Cabré
et al., 2015). Third, excess CO_2 from the atmosphere fluxing into the ocean will
cause increases in dissolved inorganic carbon (DIC) concentrations and shifts in
carbonate chemistry speciation.

How coccolithophores will respond to the above changes is subject to debate.
This is despite the vast amount of research on coccolithophores, especially within
the last 15 years. Some recent observational studies show that coccolithophores
are currently expanding in range or increasing in abundance (Winter et al.,
2013; Rivero-Calle et al., 2015; Krumhardt et al., 2016), while another reports
decreases in pelagic calcification by coccolithophores (Freeman and Lovenduski,
2015). Further, a recent mesocosm study, albeit of shorter duration, showed that
the competitive fitness of coccolithophores may be impaired by future oceanic
conditions (Riebesell et al., 2017). This raises questions as to the temporal
and geographic variation in coccolithophore responses to environmental change.
Laboratory studies have also reported mixed responses to increasing CO_2 (e.g.,
Riebesell et al., 2000; Iglesias-Rodriguez et al., 2008), temperature (e.g., Matson
et al., 2016), and light (Perrin et al., 2016; Feng et al., 2008). Feng et al. (2016),
Rouco et al. (2013), and Müller et al. (2017) considered multiple simultane-
ous effects of climate change, demonstrating that increased nutrient limitation
can strongly influence the response of coccolithphores to increasing CO_2. How-
ever, each of these studies only focused on a single strain (genetic variant) of
Emiliania huxleyi. Looking across species and morphotypes, as well as across
multiple environmental stressors, is necessary to capture broad scale responses
of coccolithophores to environmental change.

Biological syntheses on coccolithophores (e.g., Paasche, 2002; Taylor et al.,
2017) provide insights on cellular biology, physiology, and genetic aspects of coc-
colithophores (mainly *E. huxleyi*), while a recent review by Monteiro et al. (2016)

3

focuses on the purposes of phytoplankton calcification and how the cost/benefits of calcification may change in the future. Zondervan (2007) provided a qualitative review of field observations and laboratory data on environmental factors influencing organic and inorganic carbon production in coccolithophores, but a more quantitative and biogeographical approach is necessary to provide insights for Earth system modeling. Here, we combine field and laboratory data across numerous coccolithophore species and morphotypes to examine the present state and potential shifts in coccolithophore physiology and global biogeography, developing generalized mathematical relationships between coccolithophore growth and calcification across environmental gradients.

Both particulate organic carbon (POC) production via photosynthesis and particulate inorganic carbon (PIC) production via calcification by coccolithophores may be influenced by anthropogenic climate change. A coccolithophore PIC/POC ratio represents how much calcium carbonate ($CaCO_3$ or calcite) a coccolithophore produces relative to photosynthetically derived organic carbon; this is a common parameter measured in coccolithophore physiology studies (see, e.g., Findlay et al., 2011). Since coccolithophores produce roughly half of exported oceanic $CaCO_3$ (Broecker and Clark, 2009; Schiebel, 2002), the coccolithophore PIC/POC ratio is an important component of the overall rain ratio, the ratio of $CaCO_3$ produced by all open ocean calcifying organisms (coccolithophores, foraminifera, pteropods, and others) to organic carbon in sinking biogenic particles to the deep-sea floor, which strongly influences the global carbon cycle. Coccolithophore PIC/POC ratios may vary based on coccolithophore species or morphotypes within species (Figure 1; Blanco-Ameijeiras et al., 2016), but can also be highly influenced by environmental conditions (hence the large ranges and overlap within subgroups shown in Figure 1; Findlay et al., 2011; Müller et al., 2017). By quantifying coccolithophore POC production rate and relative production of PIC, it is possible to track the two most direct impacts coccolithophores have on the carbon cycle and how they may change in the future.

Despite the influence of coccolithophores on the global carbon cycle (see Hense et al., 2017) and their potential sensitivity to impending changes, only a

4

few ocean ecosystem models include a phytoplankton functional type (PFT) explicit for modeling coccolithophore growth and calcification, e.g., PlankTOM5.3 (Le Quéré et al., 2005; Buitenhuis et al., 2013a; Buitenhuis and Geider, 2010) and the NASA Ocean Biogeochemical Model (Gregg and Casey, 2007). These models simulate coccolithophore growth through nutrient, temperature, and light functions based on the commonly cultured species *Emiliania huxleyi*. However, two major challenges remain for these models. The first is to consider other coccolithophore species. While *E. huxleyi* is a substantial component of the coccolithophore community, other species also contribute to coccolithophore diversity and oceanic calcite production (Daniels et al., 2014; O'Brien et al., 2016; Buitenhuis et al., 2013b). Accounting for the range of responses across these species in model simulations is therefore important to understanding the overall role of coccolithophores in the present and future carbon cycle. The second challenge is to simulate the influence of increasing CO_2 on coccolithophore growth and calcification by identifying overarching responses from numerous, sometimes conflicting, physiological studies.

The primary goal of this study is to relate field observations of coccolithophores with experimental results of coccolithophore physiology to capture broad, cross-species conclusions about conditions in which coccolithophores thrive and how coccolithophore growth and calcification may change with future anthropogenic influences on the ocean. We aim to identify overarching patterns to guide development of an explicit coccolithophore PFT for use in an Earth system model (ESM; Le Quéré et al., 2005; Hense et al., 2017), accounting for both the production of coccolithophore organic carbon through their growth rate and the relative production of particulate inorganic carbon (via the PIC/POC ratio).

This manuscript is structured as follows. After a description of our methods in section 2, section 3 describes our current understanding of coccolithophore biogeography. Sections 4 –7 highlight relationships between coccolithophore growth/calcification and environmental conditions, as derived from physiological data compilations. In section 8 we apply these relationships in the de-

5

velopment of an empirical coccolithophore model that is driven by sea surface temperature, phosphate concentration, and the partial pressure of CO_2 at the ocean surface. The influence of light intensity was not included in our model, as its influence on coccolithophore growth and calcification was unclear based on our data compilations. Focusing on the surface ocean, in section 9 we use the empirical model to estimate current, geographically-resolved coccolithophore growth rates and relative calcification and use Community Earth System Model (CESM)-projected changes in the surface oceanic environment to estimate how these coccolithophore attributes may change over the 21st century. Finally, in section 10, we contextualize our results in light of recently observed changes in coccolithophore distribution and abundance and identify research directions that would improve projections of how these calcifying phytoplankton will respond to 21st century oceanic changes.

2. Methods

2.1. Classification of coccolithophore subgroups

We classified coccolithophore species and *Emiliania huxleyi* morphotypes (which show considerable genetic and physiological variability; Read et al., 2013; Langer et al., 2009; Cook et al., 2011, 2013) into coccolithophore *subgroups* for purposes of biogeography and to group results of physiological studies. Some numerically important coccolithophores are not included because they lack any physiological information (e.g., deep dwelling *Florisphaera profunda* or species from the *Umbellosphaera* genus). We include the following eight coccolithophore subgroups because they have been cultured in the laboratory with physiological information, as well as identified in field studies:

1) *E. huxleyi* morphotype A: This widespread morphotype, sometimes referred to as the "warm water" type of *E. huxleyi* (see, e.g., Okada and Honjo, 1973), can inhabit a variety of ocean biomes, from the subtropics to subpolar waters (see, e.g., Patil et al., 2014; van Bleijswijk et al., 1991) and shows the highest maximum growth rate in our compilation. This subgroup displays a high level

6

of plasticity in calcification (see PIC/POC range of 0.1 to 2.7 in Figure 1). *E. huxleyi* var. *corona*, although uncultured, is included in this subgroup for biogeographical purposes.

2) *E. huxleyi* morphotype B/C: This subgroup has generally been referred to as the "cold water" type of *E. huxleyi* (see, e.g., Winter, 1985; Hagino et al., 2011), generally inhabiting high latitude and upwelling oceanic regions (see, e.g., Dylmer et al., 2015). *E. huxleyi* morphotypes B, C, B/C, and D were all classified as the B/C morphotype following Hagino et al. (2005). In general, members of this subgroup have coccoliths with a relatively open central area and are more lightly calcified than morphotype A (Figure 1; Young et al., 2003).

3) Southern Ocean *E. huxleyi* B/C: This subgroup (sometimes referred to as *E. huxleyi* var. *aurorae*) is substantially less calcified than *E. huxleyi* B/C from other areas of the world ocean, having coccoliths with open central elements (Figure 1; see Young et al., 2003). Southern Ocean *E. huxleyi* B/C displays the slowest maximum growth rate within our compilation. Following a suggestion by Poulton et al. (2011) we consider this *E. huxleyi* morphotype endemic to the Southern Ocean.

4) *E. huxleyi* over-calcified: This subgroup contains *E. huxleyi* morphotype R and *E. huxleyi* morphotype A over-calcified. These morphotypes have coccoliths with heavily calcified shield elements with closed or partially fused coccolith slits (Young et al., 2003), and show similar physiological responses to increasing CO_2 (e.g., Müller et al., 2015; Iglesias-Rodriguez et al., 2008). The *E. huxleyi* over-calcified subgroup inhabits parts of the Southern Ocean and cold nutrient-rich shelf waters (Mohan et al., 2008; Cubillos et al., 2007; Smith et al., 2012, Beaufort et al., 2011).

5) *Gephyrocapsa oceanica*: This warm water coccolithophore species is well documented both in the field (e.g., Hagino et al., 2000) and in laboratory studies (e.g., Sett et al., 2014; Riebesell et al., 2000). Members of this subgroup are slightly larger than *E. huxleyi*, moderately calcified (PIC/POC $\approx$ 1; Figure 1),

7

¹⁶⁵ and show maximum growth rates within the range of *E. huxleyi* morphotypes.

6) *Coccolithus* genus: The two main species included in this subgroup, *C. pelagicus* and *C. braarudii*, are larger than *E. huxleyi* with relatively slow maximum growth rates (Figure 1). Members of the *Coccolithus* genus are moderately calcified (Figure 1) and have been observed in polar and temperate waters of the ¹⁷⁰ Northern Hemisphere (Daniels et al., 2014).

7) *Calcidiscus leptoporus*: Also a large coccolithophore (Figure 1), this species tends to be highly calcified, showing some of the largest PIC/POC ratios (despite its large size and relatively small surface area to volume ratio). Having a large geographic range, *Calcidiscus leptoporus* contributes substantially to total ¹⁷⁵ calcite production in many diverse oceanic regions (Diner et al., 2015; Baumann et al., 2004; Daniels et al., 2016).

8) *Syracosphaera* genus: Though *Syracosphaera pulchra* is the only species of this genus that has been studied in the laboratory (e.g., Fiorini et al., 2011), members of *Syracosphaera* genus are widespread in the global ocean (see, e.g., ¹⁸⁰ Guptha et al., 2005; Balestra et al., 2004; Henderiks et al., 2012; Oviedo et al., 2015). *Syracosphaera pulchra* is a relatively large species and produces some spine-bearing coccoliths (Figure 1); this species, however, may not necessarily be representative of all species within the *Syracosphaera* genus.

2.2. Coccolithophore biogeography

¹⁸⁵ We compiled data from field studies to gain an understanding of general coccolithophore biogeography. The percentage of each coccolithophore subgroup out of the total coccolithophore community was mapped, only showing subgroups numerically comprising 20% or more of the coccolithophore population, with subgroup colors corresponding to those in Figure 1. We created three ¹⁹⁰ biogeography maps: 1) coccolithophores that could be grouped into one of our *subgroups* listed above (i.e., have been cultured in the laboratory with physiological information; mainly reside in the upper to mid photic zone), 2) upper photic zone (UPZ) coccolithophores that lack physiological information, and 3)

lower photic zone (LPZ) coccolithophores (all of which lack physiological information). Points on these maps can be considered "snapshots" of coccolithophore community composition, as field studies are included regardless of the season in which they were observed (Table S1). When multiple measurements of coccolithophore abundances over the course of a year were reported, an annual mean is indicated. Further details on creating biogeographical maps and references can be found in the supplementary materials (Table S1) .

Coccolithophore biogeography was overlaid on a map of annual mean surface PIC concentration. Annual mean PIC concentration at 9 km resolution was derived from the Moderate Resolution Imaging Spectroradiometer (MODIS) Aqua, averaged over 14 years (2002–2015). The algorithm used to estimate surface PIC concentration was formulated to capture water-leaving radiances and calcite-specific backscatter unique to coccolithophore shells (Balch et al., 2005; Gordon et al., 2001). Thus, PIC concentration from satellite provides a proxy for coccolithophore calcite abundance.

2.3. Physiological studies

We compiled data from physiological studies that measured the effects of changing pCO_2, nutrient concentrations, light, and temperature on coccolithophore growth and/or calcification. All studies used in these compilations are listed in Table S2. To convert between aqueous CO_2 concentration and partial pressure of CO_2 (pCO_2), we used salinity and temperature data from each study and carbonate chemistry constants from Emerson and Hedges (2008), assuming that the fugacity of CO_2 is approximately equal to its partial pressure. We plotted these physiological data compilations against environmental gradients of CO_2, temperature, nutrients, and light. Corresponding color legends were used to associate coccolithophore subgroups shown in Figure 1 with biogeography and physiological studies.

2.4. Developing a global coccolithophore model

In order to model current coccolithophore growth and calcification in the surface ocean and project how these may change over the course of the 21st

9

century, we aimed to capture generalized coccolithophore physiology that may
be parameterized as a single PFT. We focus on surface data because the physiology studies we compiled are for coccolithophore subgroups (see section 2.1)
that generally reside in surface waters (see section 2.1). In general, marine
ecosystem components of Earth system models simulate phytoplankton growth
using a maximum phytoplankton growth rate modified by temperature, light,
and nutrient concentrations (Laufkötter et al., 2015). Because coccolithophore
photosynthesis has been shown to be carbon limited (as compared to other phytoplankton groups; Rost et al., 2003; Riebesell, 2004) we also enable the modification of coccolithophore growth rate based on pCO_2 in the surface ocean.

We used phosphate (PO_4) as a representative nutrient for our model simulations because 1) future changes in stratification clearly affect PO_4 concentration
at the surface, without being subject to other (possibly complicating) biological
influences (e.g., nitrogen fixation) and 2) PO_4 is the only source of phosphorus
for phytoplankton in Earth system models (in contrast to nitrogen, which can
be taken up by phytoplankton as nitrate or ammonia), 3) PO_4 was available
as CESM model output as well as in global compilations of oceanographic data
(see below), and (4) PO_4 availability has been shown to affect calcification (e.g.,
Müller et al., 2008; Perrin et al., 2016; Feng et al., 2016).

2.5. Driver data for our global coccolithophore model

To estimate present-day coccolithophore growth and PIC/POC, we used
modern oceanographic surface data. We obtained monthly mean sea surface
temperature and surface PO_4 concentration from GLODAP (Lauvset et al.,
2016) and monthly mean smoothed surface pCO_2 from Landschützer et al.
(2015).

To project long-term changes in coccolithophore growth and calcification
we used ESM-simulated environmental variables over the 21st century. In order to capture *long-term* changes in the surface ocean environment (outside of
natural variability), we used output from the Community Earth System Model
Large Ensemble (CESM-LE) simulations (Kay et al., 2015; Lovenduski et al.,

2016; Krumhardt et al., 2017). Briefly, CESM (version 1) was run with ocean, land, sea ice, and biogeochemistry components, starting with a long, preindustrial control simulation until quasi-equilibrium was reached. The first ensemble member was started from these initial conditions and integrated forward in time from 1850 to 2100, driven first by historical forcing, then RCP 8.5 to simulate future conditions. Thirty-three other ensemble members were branched off of the first ensemble member at 1920 with small ($10^{-14\circ}$C) changes in air temperature. While each ensemble member simulation is identically forced, the phasing of natural (internal) climate variability differs among ensemble members. The ensemble mean of simulated variables (e.g., sea surface temperature, nutrient concentrations) captures long-term, forced trends, while the variance across ensemble members quantifies the influence of natural climate variability on a particular variable. Here, we focus on the ensemble mean to project long-term effects of anthropogenic climate change on the coccolithophore environment, and use variation across ensemble members to evaluate where changes are most robust.

We used CESM-LE mean monthly output on sea surface temperature, surface PO_4 concentration, and surface pCO_2 to project how the coccolithophore environment may change from present to end of the 21st century. Decadal averages of each of these variables for each month were made for present day conditions (2006–2015) and future, end-of-the-century conditions (2091-2100) for each ensemble member, resulting in present day and end-of-the-century monthly climatologies. We applied this monthly data in our empirical model to estimate coccolithophore growth rate and PIC/POC for these two time periods for each CESM-LE member. To analyze our data, we averaged monthly coccolithophore growth rates and PIC/POC ratios over the growing season: June, July, August in the Northern Hemisphere and December, January, February in the Southern Hemisphere. We compared present-day coccolithophore growth rate and PIC/POC from our coccolithophore model driven by modern oceanographic data with results driven by present-day CESM-LE data (see Supplementary section). Geographically-resolved differences in growing season

coccolithophore growth rate and PIC/POC ratio between the end and the beginning of the century were used to demonstrate how these attributes may change. We demonstrated statistical significance of 21st century changes by calculating where ensemble mean differences exceeded two times the standard deviation of the differences across ensemble members (i.e., where signal-to-noise ratio exceeded two). Data are presented in maps that show growing seasons in each respective hemisphere.

We also tested individual effects of drivers (CO_2, PO_4, temperature). By holding two of the drivers constant at present day values, we could observe the effect of a single driver. In the case of CO_2 and PO_4 limitation on growth rate, we isolated the limiting effect of each of these (i.e., only CO_2 could limit growth when testing the effects of CO_2 changes and only PO_4 could limit growth when testing the effects of changes in PO_4 concentration). Lastly, we ran the model with all drivers active to demonstrate their combined effects and relative importance on coccolithophore growth rate and PIC/POC to surface ocean changes over the 21st century. We relate these changes to the current biogeography of coccolithophore subgroups.

3. The current biogeography of coccolithophores

Coccolithophores are widespread throughout the global ocean, from high latitudes to the tropics (from ∼70°N to ∼60°S), with subgroups specialized for growth in nearly every oceanic environment (Figure 2a). Mean annual surface PIC concentrations underlying coccolithophore subgroup biogeography Figure 2a in combination with uncultured species (shown in Figure 2b, c) show that areas where PIC concentration is low (tropic and subtropics) tend to harbor more diverse coccolithophore assemblages. This is in contrast to temperate and subpolar regions, which have the highest concentrations of PIC and are mostly dominated by only one or two coccolithophore species.

Indeed, though *E. huxleyi* is ubiquitous throughout the global ocean, this species is especially abundant at high latitudes (>45°; Figure 2; Charalam-

12

popoulou et al., 2016; Poulton et al., 2014, 2011; Dylmer et al., 2015; Balch et al., 2016). In the North Pacific *E. huxleyi* morphotype B/C dominates, with other species such as those from the *Coccolithus* genus also present in significant numbers (Figure 2a; Tsutsui et al., 2016; Hagino et al., 2005). The North Atlantic appears to be strongly dominated by *E. huxleyi* morphotype A south of 60°N, but changes to an assemblage co-dominated by *E. huxleyi* B and *C. pelagicus* at latitudes >60°N (Figure 2a; van Bleijswijk et al., 1991; Charalampopoulou et al., 2011; Dylmer et al., 2015; Daniels et al., 2014). The assemblage in the far North Atlantic (>60°N) resembles that of the North Pacific between 45 and 60°N. Despite the numerical dominance of *E. huxleyi*, larger species such as *C. pelagicus* can be major contributors to calcite production relative to the smaller *E. huxleyi* (see Figure 1 for approximate sizes; Daniels et al., 2014). Thus, the biogeography presented in Figure 2 focuses on cell counts and may not be representative of proportionality of coccolithophore biomass or calcite content. Indeed, minor numerical contributions from species such as *C. pelagicus* may have a disproportionately large contribution to the high surface PIC measured by satellite for subpolar or upwelling regions (Figure 2a; Daniels et al., 2014).

In contrast, coccolithophores in the Southern Ocean are nearly exclusively *E. huxleyi*, with individual morphotypes showing some remarkable consistency across Antarctic Circumpolar Current frontal zones (see gray lines on Figure 2a). North of the Subtropical Fronts, the *E. huxleyi* over-calcified subgroup generally dominates the assemblage (Figure 2a; Mohan et al., 2008; Cubillos et al., 2007). Just south of South Subtropical Front (but north of Subantarctic front), *E. huxleyi* morphotype A becomes increasingly present (Cubillos et al., 2007; Patil et al., 2014). South of Subantarctic Front, the coccolithophore assemblage changes to a stark dominance of Southern Ocean *E. huxleyi* morphotype B/C (Poulton et al., 2011; Mohan et al., 2008; Cubillos et al., 2007; Findlay and Giraudeau, 2000; Charalampopoulou et al., 2016). The Southern Ocean morphotype of *E. huxleyi* B/C, composing up to 99% of the coccolithophore assemblage in this southernly zone (Findlay and Giraudeau, 2000; Charalam-

popoulou et al., 2016), is lightly calcified, producing ∼50% less calcite than other *E. huxleyi* morphotypes (Poulton et al., 2013; Charalampopoulou et al., 2016; Müller et al., 2015). Even so, the high concentration of surface PIC in the Southern Ocean (Figure 2) suggests *E. huxleyi* could be present in high numbers (indeed 4 x 10^6 cells per liter is reported by Mohan et al., 2008) or the satellite PIC algorithm is overestimating PIC due to the unique reflectance properties of Southern Ocean *E. huxleyi* morphotype B/C (Holligan et al., 2010).

In contrast to this lightly calcified, monospecific assemblage in this cold Antarctic region, tropical and subtropical coccolithophores that have been isolated and studied tend to have higher midpoint PIC/POC ratios. With regard to *E. huxleyi*, morphotype A (which we grouped with var. *corona*) is observed in the subtropical gyres (Cortés et al., 2001) with coexistence of morphotypes A and B in upwelling and coastal regions (Ziveri et al., 1995; Saavedra-Pellitero et al., 2010; Hagino et al., 2000). *G. oceanica* commonly resides in regions with warm, turbulent surface waters, such as the equatorial Pacific currents, the western Mediterranean, or along tropical coastlines (Andruleit et al., 2003; Hagino and Okada, 2004; Oviedo et al., 2015). *C. leptoporus* is also present in some of the same areas as *G. oceanica*, preferring warmer, eutropic environments (Figure 2a; Hagino and Okada, 2004). However, many dominant species in these warm oceanic regions have not been studied in the laboratory, and thus, are not included in the main coccolithophore subgroups listed in section 2.1, shown in Figure 1, or mapped in Figure 2a. This is especially true for species belonging to the *Umbellospheara* genus in the UPZ (Figure 2b) and for *Florisphaera profunda* in the LPZ (Figure 2c). In addition to the species shown on the maps in Figure 2, there are many more that are present in small percentages. For example, a survey of coccolithophores at a site in the subtropical North Atlantic near Bermuda found 55 coccolithophore taxa present, though *E. huxleyi* was the most abundant species (Haidar and Thierstein, 2001). In agreement, O'Brien et al. (2016) combined an extensive global compilation of coccolithophore species with environmental data to create a neural network that predicts the highest coccolithophore diversity in low latitudes.

14

Most laboratory studies of coccolithophore species have focused on two sub-types of *E. huxleyi*, morphotype A and morphotype R (see Table S2). The well-studied *E. huxleyi* morphotype A is geographically widespread. Morphotype R, which we group with over-calcified morphotype A on our biogeography map (Figure 2a), is limited in geographic distribution to waters immediately surrounding New Zealand (see Figure 2a for isolation locations of strains used in, e.g., Iglesias-Rodriguez et al., 2008; Kottmeier et al., 2016; Rokitta and Rost, 2012) and a few other productive coastal regions (Figure 2a; Beaufort et al., 2011). Also evident from compilations presented in Figure 2b and c, numerous UPZ and LPZ species that are major components of the coccolithophore community have not been studied in controlled laboratory settings and their responses to anthropogenic climate change remain unknown.

Distributions of the coccolithophore subgroups defined here loosely follow boundaries of physical and chemical properties such as sea surface temperature, macronutrient concentrations, dissolved inorganic carbon concentration, and salinity (see Figure 2 compared to, e.g., color plates in Sarmiento and Gruber, 2006). As the oceanic environment evolves with anthropogenic climate change, we can expect shifts in these biophysical properties (Gruber, 2011). In the following sections we compile numerous physiological studies on major coccolithophore subgroups shown in Figures 1 and 2a to explore how their distributions and physiology may change with relevant changes the oceanic environment (changes in temperature, light, nutrient availability, and CO_2 concentration). In Section 8 we combine these relationships within a mathematical modeling framework suitable for Earth system modeling.

4. Physiological responses to changes in CO_2 concentration

As anthropogenic CO_2 inundates the ocean surface, the concentration of DIC increases (increasing pCO_2, as well as bicarbonate, HCO_3^-, concentration), while alkalinity remains the same. This causes a shift in the carbonate chemistry equilibrium, resulting in higher hydrogen ion (H^+) concentrations (decreas-

15

ing pH) and lower calcium carbonate saturation states. An increase in pCO_2 could benefit coccolithophore photosynthesis because coccolithophores have a relatively inefficient carbon concentrating mechanism, and thus can be carbon limited compared to other phytoplankton (Bach et al., 2013; Riebesell, 2004; Reinfelder, 2011). Further, coccolithophore calcification may respond positively to increasing HCO_3^- ions, the primary substrate for calcification, while simultaneously being inhibited by increasing H^+ ions (the substrate-inhibitor concept; see Bach et al., 2015). Therefore, future changes in carbonate chemistry could have both detrimental and beneficial effects for coccolithophores. In this section, we examine physiological studies that address the potential effects of anthropogenic CO_2 on coccolithophore growth rate and calcification (PIC/POC).

4.1. Growth rate and CO_2

Most studies have investigated the effect of *increased* CO_2 concentrations on coccolithophore growth. Thus, when combining many studies across culturing conditions and coccolithophore species, morphotypes, and strains, most of the growth rate measurement data were clustered around high CO_2 concentrations (i.e., there was a lack of growth rate measurements at low CO_2 concentrations). Unconstrained, equally-weighted Michaelis-Menten fits to these data resulted in negative half saturation constants, which have no physical interpretation. To overcome this limitation, we binned growth rate data in 50 μatm pCO_2 bins following Rivero-Calle et al. (2015), calculating the median, mean, maximum and minimum growth rates in each bin (Figure 3 and Figure S1). We used these binned data to calculate growth rate-specific CO_2 uptake kinetics.

Coccolithophores may modify their growth rate and cellular POC content in response to ambient CO_2 concentration in seawater (e.g., see Riebesell et al., 2000; Langer et al., 2006; Iglesias-Rodriguez et al., 2008). Growth rates based on cell concentrations do not account for the changing amount of POC contained within coccolithophore cells and biomass. Therefore, in addition to deriving a relationship for traditional cell-based growth rates as a function of CO_2 concentration (see Figure S1 for a compilation of cell-based growth rate as a function

16

of pCO$_2$ and Figure S2 for a comparison of the two methods), we also created a function using POC-based growth rates (shown in Figure 3). POC-based growth rates are normalized to cellular POC content in cultures in which pCO$_2$ was closest to 390 μatm (i.e., cultures grown under modern-day, ambient atmospheric CO$_2$; actual range in our data compilation: 322 – 431 μatm) so that:

$$\mu_{POC} = \mu_{cell} \cdot \left(\frac{POC_{cell}}{POC_{cell(ambientCO_2)}} \right) \qquad (1)$$

where μ_{POC} is the POC-based growth rate (d^{-1}), μ_{cell} is the cell-based growth rate (d^{-1}), POC$_{cell}$ is the POC per cell (pg C cell^{-1}), and POC$_{cell(ambientCO2)}$ is the POC per cell at modern-day, ambient pCO$_2$ (pg C cell^{-1}). This process is similar to a normalization to cell volume suggested by Müller et al. (2017) to isolate the effects of nutrient limitation on *E. huxleyi* apart from CO$_2$ changes. Using a POC-based growth rate allows the direct use of a PIC/POC ratio to calculate the precipitation rate of PIC (calcification) by coccolithophores relative to their growth in biomass, which is beneficial to modeling efforts. POC-based and cell-based growth rate-specific CO$_2$ uptake kinetic parameters are listed in Table 1. In general, estimates of K$_{CO2}$ are smaller when using cell-based growth rates (Table 1; Figure S2).

The compilation of growth rates under a variety of CO$_2$ concentrations shows the large range of measured coccolithophore growth rates in cultures (Figure 3a). This variation is not only due to differences in culturing conditions (nutrients, light, temperature) but also to inter-species and inter-strain variability. Growth rates of some coccolithophores appear limited at low CO$_2$ concentrations (see Figure 3b–g), but overall we observe large plasticity in growth as a function of CO$_2$. This data compilation is somewhat biased to the more commonly cultured A morphotype of *E. huxleyi*, but this group also has the largest spread in growth rates across relevant CO$_2$ concentrations (Figure 3c), with some studies showing substantial carbon limitation at low CO$_2$ concentrations (e.g., see Rost et al., 2003). Growth of *G. oceanica* also appears to be carbon limited at low CO$_2$ concentrations (Figure 3e; Sett et al., 2014; Rickaby et al., 2010). Other less

17

widespread species, such as highly calcifying *Coccolithus pelagicus*, maintain relatively slow growth rates regardless of the CO_2 concentration, suggesting CO_2 is not a limiting factor on their growth. On the other hand, *C. leptoporus* and *E. huxleyi* morphotype R show slightly increasing POC-based growth rates as CO_2 increases (Figure 3b and f). This relationship is not evident in Figure S1, where cell-based growth rates are plotted as a function of CO_2.

In general coccolithophores use HCO_3^- for calcification and CO_2 for photosynthesis (Bach et al., 2013; Rost et al., 2003). If CO_2 becomes limiting, coccolithophores can supplement their photosynthetic carbon needs with HCO_3^- (Bolton and Stoll, 2013; Bach et al., 2013; Rost et al., 2003). Coccolithophores rely on diffusive CO_2 uptake as a carbon source for photosynthesis and actively transport HCO_3^- through the cell membrane for calcification (and photosynthesis if CO_2 is limiting; Bolton and Stoll, 2013; Nimer and Merret, 1992; Bach et al., 2013). Increasing CO_2 concentrations could relieve cells of the need for active carbon (HCO_3^-) transport for photosynthesis. Kottmeier et al. (2016) demonstrated that increasing H^+ ions triggers a decline in HCO_3^- uptake relative to CO_2 uptake in *E. huxleyi* morphotype R. The excess energy saved from not having to actively transport carbon could then be used to supplement growth. This could be the reason that numerous studies have observed increases in cellular POC content as a result of increasing CO_2 concentration (e.g., Sett et al., 2014; Riebesell et al., 2000). Also worth mentioning, as the process of calcification produces CO_2, it could serve as a carbon concentrating mechanism for photosynthesis (Buitenhuis et al., 1999), although some studies do not support this hypothesis (for a summary see Monteiro et al., 2016). Similarly, calcification, especially during a bloom, could bioengineer the adjacent environment to buffer pH, countering alkalinization caused by photosynthesis and preventing CO_2 from becoming limiting (Flynn et al., 2016).

4.2. PIC/POC and CO_2

Numerous studies have measured coccolithophore PIC/POC ratios under varying CO_2 concentrations (see Table S2). We compiled these into a com-

prehensive dataset to capture a robust relationship between coccolithophore PIC/POC and pCO$_2$ (Figure 3). A least squares line was fit to the data over a range of 0 to 1000 μatm CO$_2$. We limited our regression to this CO$_2$ concentration range to reflect realistic surface ocean pCO$_2$ future projections and because most of the compiled data fell within this range (see small corner plot on Figure 3a). We find that the production of PIC in relation to POC decreases under increasing CO$_2$ (Figure 3h). A linear regression of all coccolithophore subgroups provides this linear relationship (p = 0.0005) :

$$\frac{PIC}{POC} = -0.000456 \cdot pCO_2 + 1.21 \tag{2}$$

where pCO$_2$ is in units of μatm, or

$$\frac{PIC}{POC} = -0.0133 \cdot CO_{2(aq)} + 1.22$$

where CO$_{2(aq)}$ is in units of μmol kg^{-1}. The slope and y-intercept are slightly different from those of Findlay et al. (2011) who compiled only data for *E. huxleyi* PIC/POC ratios as a function of CO$_{2(aq)}$ (slope = -0.0097; y-intercept = 0.9654). According to our linear regression, coccolithophore PIC/POC could be expected to decrease by 37% from preindustrial pCO$_2$ (280 μatm) to 1000 μatm. Individual coccolithophore subgroups show variable PIC/POC responses to increasing CO$_2$ (Figure 3i–n). While *G. oceanica* and *E. huxleyi* morphotype A show steady declines in PIC/POC as CO$_2$ increases, *E. huxleyi* morphotype R shows no response. However, other effects of climate change could influence the PIC/POC response such as changes in sea surface temperature, nutrient availability, or mixed layer irradiance (Boyd et al., 2008; Charalampopoulou et al., 2016).

5. Physiological responses to changes in temperature

5.1. Growth rate and temperature

The relationship between temperature and coccolithophore maximum growth rate is presented in Figure 4a. Using an extensive data compilation, Fielding

19

(2013) demonstrated that a power function best describes the relationship between *E. huxleyi* maximum growth rate and temperature from 0°C to 27°C

520 (shown in Figure 4a). This function was formulated based only on data for *E. huxleyi*, which is smaller than most coccolithophore species. According to the metabolic theory of ecology, other (larger) coccolithophores should have lower maximum growth rates than *E. huxleyi* (Fielding, 2013), thus the power function should encompass all coccolithophore growth rates. In agreement, non-*E.*

525 *huxleyi* species are within the maximum growth rates specified by the power function (Figure 4a). Other models have used Q10 factors to describe temperature growth limitation in phytoplankton (Moore et al., 2004; Tyrrell and Taylor, 1996). Neither the power function nor Q10 factor encode a decrease in growth rate with increasing temperature beyond a thermal optimum, which

530 has been observed in coccolithophores and other phytoplankton (Boyd et al., 2013; Buitenhuis et al., 2008). A model with generalized PFTs (each PFT describing a variety of species) assumes that the warm water-adapted species of each PFT will continue to flourish as waters warm, with growth rates continuing to increase with temperature. However, under extreme warming events, which

535 could become more frequent with anthropogenic climate change, this may not be realistic if temperatures exceed optima for all phytoplankton species that a PFT describes.

Indeed optimum growth temperatures could be an important factor controlling the distribution of different coccolithophore groups in the ocean (Buiten-

540 huis et al., 2008; Paasche, 2002). Coccolithophores of the genus *Coccolithus* have fast growth rates at lower temperatures, consistent with their adaptation to colder oceanic environments (Figure 2a; Buitenhuis et al., 2008; Daniels et al., 2014). The warm water species, *G. oceanica* (Figure 2a; Buitenhuis et al., 2008), displays a growth optimum at temperatures >25°, while *E. huxleyi* shows

545 high growth rates (>0.8 d^{-1}) at a large range of temperatures (maximum at ∼20°C), consistent with a broad geographical distribution (Figure 2a). As the sea surface warms, coccolithophores with lower temperature optimums (and lower maximum growth rates; e.g., *Coccolithus* genus) may shift their range

northward and/or be replaced by species with high growth rates in warmer

⁵⁵⁰ waters. The power function encompasses these shifts within a generalized coc-colithphore PFT, supported by data compiled by Fielding (2013) and Buitenhuis et al. (2008), at least up to 27°C, the maximum temperature tested in these studies.

5.2. PIC/POC and temperature

⁵⁵⁵ We compiled measured coccolithophore PIC/POC ratios under various cul-ture temperatures, ensuring data were independent of other factors that could influence PIC/POC (CO_2 concentration, nutrient status; Figure 4b). The com-pilation of data across coccolithophore subgroups indicates that the highest PIC/POC ratios are observed between 15°C and 20°C. As the dataset was

⁵⁶⁰ heavily weighted around typical culturing temperatures for *E. huxleyi* (15°C - 20 °C; Figure 4b), we binned the data on PIC/POC as a function of temperature into 5°C bins to see if any overarching trends were evident (see box and whisker symbols in Figure 4b). Feng et al. (2016) fit a PIC/POC-temperature function to data from *E. huxleyi* A (thin black line on Figure 4b). However, only the

⁵⁶⁵ maximum values in the binned data displayed a significant fit to this function, and the relationship shows an unrealistic drop-off in PIC/POC at temperatures ¿20°C (see red line on Figure 4b). Indeed, PIC/POC ratios may change dra-matically (>2 fold) with temperature for some coccolithophore subgroups, while others show little or no response.

⁵⁷⁰ Studies that specifically address the influence of temperature on PIC/POC report mixed results. For instance, Matson et al. (2016) and Feng et al. (2016) showed that PIC/POC ratios in an *E. huxleyi* R morphotype and an A mor-photype, respectively, increased with increasing temperature during exponential growth, showing minimum PIC/POC ratios at low temperatures. However, an-

⁵⁷⁵ other strain used in the Matson et al. (2016) study, a subtropical *E. huxleyi* A morphotype, showed little response to temperature change with respect to the PIC/POC ratio. Moreover, Rosas-Navarro et al. (2016) found that PIC/POC shows a minimum at optimal growth temperature (between 20 and 25°C) for

21

three strains of *E. huxleyi* morphotype A isolated from a warm current off the coast of Japan. Similarly, De Bodt et al. (2010) observed PIC/POC ratios above 2 for an *E. huxleyi* morphotype A isolate when grown at 13° C, but reported PIC/PIC ratios <1 in cultures grown at 18°. Also, Gerecht et al. (2014) found that the colder water species, *C. pelagicus*, decreased its PIC/POC ratio under high temperatures.

Despite these inconsistencies, a number of studies have reported that high latitude coccolithophores have low PIC/POC ratios (Müller et al., 2015) or low coccolith calcite content (Charalampopoulou et al., 2016). Further, decreasing calcification at low temperatures has been demonstrated for *E. huxleyi* isolates from the Southern Ocean (Feng et al., 2016; Matson et al., 2016), the North Atlantic (Watabe and Wilbur, 1966) and the subarctic North Pacific and Arctic Oceans (Saruwatari et al., 2016). Therefore, we opted to use a simple linear equation for describing the relationship between coccolithophore PIC/POC and colder temperatures (fit to data for temperatures <11°C: p=0.05; r^2=0.49). In general, however, we felt most of the data describing the influence of higher temperatures on PIC/POC was unclear. Thus, we limit the temperature influence on PIC/POC to colder waters. For warmer waters with temperatures above this threshold, we hold PIC/POC constant, though there is some evidence that high temperatures (beyond a temperature optimum) may also lead to decreased calcification (Watabe and Wilbur, 1966; Feng et al., 2016; De Bodt et al., 2010; Gerecht et al., 2014). Further research on the influence of temperature on coccolithophore PIC/POC over a wide range of temperatures and on variety of coccolithophore subgroups is necessary to develop a more thorough understanding of this relationship.

6. Physiological responses to changes in nutrient limitation

6.1. Growth rate and nutrients

Nutrient limitation is an important factor controlling the growth and distribution of phytoplankton. In ESMs, phytoplankton growth rates are modified

22

by nutrient concentrations. These models prescribe half-saturation constants for Michaelis-Menten uptake kinetics (Laufkötter et al., 2015). A smaller half saturation constant (K_M) indicates better competitive ability for a nutrient at low concentrations. A fractional nutrient limitation term modifies the maximum growth rate of phytoplankton:

$$\mu = \mu_{max} \cdot \left(\frac{N}{N + K_M} \right) \tag{3}$$

where N is the nutrient concentration, K_M is the half saturation constant for that nutrient, μ_{max} is the maximum growth rate, and μ is the nutrient-modified growth rate. We compiled half saturation constants for NO_3, NH_4, PO_4, and Fe measured in the laboratory for coccolithophores (Table 2). While our compilation includes only single estimates of half-saturation constants for NH_4 and Fe, estimated half saturation constant ranges for NO_3 and PO_4 are 0.1 – 13.71 μM and 0.051 – 0.31 μM, respectively. Excluding an outlier (the K_M for NO_3 measured by Feng et al. (2016)), all half-saturation constants are approximately 1μM or below, indicating adaptation to oligotrophic conditions and helping to explain coccolithophore success under nutrient limitation observed in field studies.

Indeed, field observations can provide insights on the effect of nutrients on coccolithophore growth. Coccolithophores can account for >20% of phytoplankton carbon in severely nutrient-limited oligotrophic gyres (Poulton et al., 2007), indicating competitive fitness under long-term nutrient limitation. At higher latitudes (>45° N or S), however, coccolithophores can be present in much higher numbers (see PIC concentration proxy in Figure 2a). Nutrient concentrations could be an important factor in triggering coccolithophore blooms in these regions, as coccolithophores can outcompete larger phytoplankton when nutrients become limiting. In a modeling study, Tyrrell and Taylor (1996) found that low phosphate concentrations ($< \sim$0.2 μmol kg^{-1}) with plentiful nitrate were ideal to simulate a bloom (N:P > 20), but a compilation of field measurements indicated that high N:P ratios were not essential to the development

of coccolithophore blooms (Lessard et al., 2005). Additionally, coccolithophore species (especially *E. huxleyi*) are capable of using a wide variety of organic nutrients, such as glycine, adenoside triphosphate, or urea, which would increase their competitive ability where inorganic nutrients are low (Benner and Passow,

640 2010). In any case, efficient nutrient uptake kinetics allow coccolithophores to outcompete other phytoplankton where nutrients are sparse (Tyrrell and Taylor, 1996; Riegman et al., 2000; Perrin et al., 2016).

6.2. PIC/POC and nutrients

To capture the effect of nutrient limitation on coccolithophore PIC/POC,

645 we assembled studies that measured PIC/POC in cultures grown under PO_4 limiting (N:P > 150) and NO_3 limiting (N:P < 1.5) conditions compared with cultures grown under nutrient replete conditions (i.e., cultures in exponential growth; Figure 5). On average, PIC/POC increased by 37% from P-replete conditions to P-limited conditions and by 25% from N-replete conditions to

650 N-limited conditions. Though PIC/POC increases are seen under both P limitation and N limitation, severe P limitation is known to produce the biggest increases in the number of coccoliths per cell (Paasche, 2002) and cellular calcium content (a six fold increase; see Müller et al., 2008). Unfortunately, we could not locate any studies addressing the effect of Fe limitation on coccol-

655 ithophore PIC/POC.

Müller et al. (2008) described a possible reason why calcification relative to photosynthesis may increase under nutrient limitation. As coccolithophores are single-celled organisms, they pass through a series of cell division phases: G1, S (DNA synthesis), G2, and M (mitosis) phases. When growth is lim-

660 ited by nutrients, cells spend more time in the G1 phase; this is the primary phase during which calcification is carried out. Calcification is more limited by light than by nutrients, and therefore, cells in which growth has been slowed by nutrient limitation can continue to calcify (see also Monteiro et al., 2016; Sheward et al., 2017). Under future anthropogenic climate change, warming-

665 induced ocean stratification will constrain nutrient availability in the photic zone

24

(Cabré et al., 2015; Gruber, 2011), which suggests an increase in coccolithophore PIC/POC.

Since we use PO_4 as a representative nutrient in our coccolithophore model (see Methods), we address nutrient limitation in our model using a simple linear relationship between PIC/POC and growth rate under P-replete and P-limited conditions. This relationship is based on mean values from our compilation of studies shown in Figure 5a and listed in Table S2. The 37% mean increase in PIC/POC described above was accompanied by a P-limited growth rate that was 33% of the P-replete growth rate (mean growth rates were 0.29 d^{-1} and 0.88 d^{-1} under P-limited and P-replete conditions, respectively). Coccolithophore PIC/POC remains unchanged when PO_4 concentration is not limiting to growth.

7. Physiological responses to changes in irradiance

7.1. Growth rate and irradiance

Numerous studies have measured the influence of irradiance on coccolithophore growth rates (or other indicators of photosynthetic activity; see Figure 6a). Despite the fact that most of the compiled experiments were performed on one coccolithophore subgroup (*E. huxleyi* morphotype A), maximum metabolic rates occurred at a wide range of light intensities (between roughly 3 and 35 mol quanta m^{-2} d^{-1}; see orange lines in Figure 6a; Nanninga and Tyrrell, 1996; Balch et al., 1992). Overlapping with this range, critical irradiance for bloom formation is between 25 and 150 μmol quanta m^{-2} s^{-1} according to a probability density function based on satellite-derived coccolithophore bloom maps and global climatological maps of nutrients and physical variables such as temperature and irradiance (see hatched area on Figure 6a with top x-axis; Iglesias-Rodríguez et al., 2002). Unlike other phytoplankton, coccolithophores do not appear to experience photoinhibition, even at very high (> 1700 μmol quanta m^{-2} s^{-1}) light intensities (Balch et al., 1992; Nanninga and Tyrrell, 1996). We fit Michaelis-Menten curves to the data sets that encom-

passed the data: Nanninga and Tyrrell (1996) and Balch *et al.* (1992; orange lines on Figure 6a). According to these regressions, half-saturation light levels are between 1.8 and 52 mol quanta m^{-2} d^{-1}. While light level could be an important factor in initiating coccolithophore blooms, this compilation of data suggests that coccolithophore growth responses to irradiance are quite variable

700 and may be overridden by other environmental conditions (e.g., temperature; Zondervan, 2007).

7.2. PIC/POC and irradiance

The effect of light on PIC/POC is complex (see summary in Zondervan, 2007). We plotted PIC/POC as a function of irradiance (Figure 6b). As en-

705 ergy is required for calcification, it is generally expected that coccolithophore production of PIC should be dependent on light. While numerous studies have observed increases in cellular calcium carbonate content with increasing irradiance (Perrin et al., 2016; Langer et al., 2007; van Bleijswijk et al., 1994; Nimer and Merret, 1993; Zondervan et al., 2002), others report the opposite trend

710 (Feng et al., 2008; Rokitta and Rost, 2012).

The contrasting functions of coccoliths within the various coccolithophore groups may explain the lack of an overarching relationship between irradiance and PIC/POC. For instance, for lower photic zone species, such as *Florisphaera profunda* (Figure 2c), coccoliths may help focus scarce light on the coccol-

715 ithophore cell (for an overview, see Monteiro et al., 2016). The flower-like forms of *F. profunda* and *Gladiolithus flabellatus* (see images in Young et al., 2003), both prevalent LPZ species (Figure 2c), may reflect this function. In contrast, coccoliths may also protect the cell from photodamage, e.g., in surface water blooms (Paasche, 2002; Monteiro et al., 2016). By acting as a shade for excess

720 photosynthetically active radiation and UV light, coccoliths help modulate light transmission into the coccolithophore cell. For example, calcified *E. huxleyi* displayed 3.5 times faster growth rates than non-calcified cells of the same strain when exposed to UV light (Xu et al., 2016). Therefore, each coccolithophore species or morphotype may display distinct optima in regard to calcification un-

26

der various light intensities, while some coccolithophore PIC/POC ratios may not be greatly influenced by irradiance at all. Due to the ambiguity of irradiance influence on both growth rate and calcification, we do not include the effect of irradiance in our generalized coccolithophore model.

8. Summary of generalized empirical coccolithophore model

730   We aim to capture the most prominent features of coccolithophore biogeography and environmental modulation of coccolithophore growth rate and PIC/POC in our generalized coccolithophore model. We model the effects of temperature, CO_2, and nutrient availability (using PO_4 as a representative nutrient – see Methods) on growth rate and PIC/POC of coccolithophores (shown

735 in red on Figure 7). To model coccolithophore growth rate, we first calculated the maximum growth rate at a given temperature according to the Fielding (2013) power function:

$$\mu_{max} = 0.1919T^{0.8151} \tag{4}$$

where μ_{max} is maximum growth rate in days^{-1}and T is temperature in °C. Maximum temperature-based growth rate is then modified based on PO_4 or

740 CO_2 limitation using the minimum of fractional limitation terms:

$$CO_2lim = \left(\frac{pCO_2}{pCO_2 + K_{pCO2}}\right) \tag{5}$$

and

$$PO_4lim = \left(\frac{PO_4}{PO_4 + K_{PO4}}\right) \tag{6}$$

so that:

$$\mu = \mu_{max} * min(CO_2lim, PO_4lim) \tag{7}$$

where μ_{max} is the temperature-modified growth rate and μ is the realized growth rate, both in days^{-1}. We used the mean K_{pCO2} for POC-based growth rate of 51.4 μatm (Table 1) and a mean K_{PO4} of 0.17 μM (average of K_{PO4} values listed

27

in Table 2). It is important to keep in mind that growth rate estimates are in the absence of competition with other phytoplankton, and therefore represent a high-end estimate or *potential* growth rate given environmental conditions.

PIC/POC was modeled by first calculating a baseline PIC/POC (PIC/POC$_1$) value based on temperature. At temperatures below 11°C, PIC/POC decreases linearly with temperature; baseline PIC/POC is constant at temperatures >11°C, formulated as:

$$\frac{PIC}{POC}_1 = 0.104 \cdot T - 0.108, \quad T < 11 \tag{8}$$

and

$$\frac{PIC}{POC}_1 = 1, \quad T \geq 11$$

where T is temperature (shown on Figure 4 by dashed black line). Secondly, PIC/POC is adjusted based on the slope of the linear relationship between PIC/POC and pCO$_2$ by the equation

$$\frac{PIC}{POC}_2 = -0.000456 \cdot pCO_2 + \frac{PIC}{POC}_1 + 0.21 \tag{9}$$

For temperatures warmer than 11°C, the above equation is the same as the regression line in Figure 3b and the equation 2. Finally, PIC/POC is modified upwards in regions of P-limitation by a linear equation derived from averaging the results summarized in Figure 5a on changes in PIC/POC as a result of PO$_4$ limitation:

$$\frac{PIC}{POC}_{final} = -0.48 \cdot PO_4 lim + \frac{PIC}{POC}_2 + 0.48 \tag{10}$$

Under PO$_4$-replete conditions, $PO_4 lim$ is 1 and PIC/POC$_2$ is not changed by this equation (i.e., PIC/POC$_{final}$ is equal to PIC/POC$_2$).

In the following section, we use this model to estimate contemporary coccolithophore growth rates and PIC/POC in the surface ocean using oceanographic data. Next, we use output from the CESM-LE to project how changes in the surface ocean over the 21st century following the business-as-usual emission scenario (RCP 8.5) will affect coccolithophore growth and PIC/POC.

9. Coccolithophore model results

9.1. Current coccolithophore growth and PIC/POC

Modeled coccolithophore growth rate and PIC/POC maps for the growing season based on contemporary oceanographic datasets (Figure 8) indicate that the fastest coccolithophore growth rates occur in the equatorial regions, where high temperatures and adequate nutrient (represented by PO_4 in our model) availability allow potential coccolithophore growth rates to be greater than 1.6 d^{-1}. This is likely an overestimate, as competition for nutrients and light with other phytoplankton and other limitations not considered here (e.g., Fe limitation) could substantially affect growth rates in these regions. Within the subtropical gyres strong nutrient limitation leads to slow coccolithophore growth rates, estimated between 0.1 and 0.4 d^{-1}. Mid-latitude regions have moderate growth rates between 0.6 and 1.2 d^{-1}, which are typically what is observed in culture at today's CO_2 levels (Figure 3a; see also Blanco-Ameijeiras et al., 2016). The effect of pCO_2 on potential coccolithophore growth rates is minor. In general, CO_2 limitation outweighs PO_4 limitation only in regions where macronutrients are plentiful, e.g., the far North Pacific and Southern Ocean (not shown). However, phytoplankton in these regions are frequently iron-limited (iron limitation is not considered in our model), which could which could confound the potential physiological impact of C-limitation.

Though it is difficult to evaluate simulated potential growth rate estimates, current coccolithophore PIC/POC ratios estimated by our model (Figure 8b) can cautiously be compared to the biogeographic distribution shown on Figure 2a, as the colors of the dots represent midpoint PIC/POC values for cultured

29

coccolithophores presented in Figure 1. Indeed, colored dots mapped in Figure 2a generally match the PIC/POC estimates shown in Figure 8b. PIC/POC ratios are highest in subtropical gyres, ranging between 1 and 1.5, and lowest at the poles. Our model estimates that coccolithophore PIC/POC is between 0.9 and 1.3 for temperate and sub-polar regions of the Northern Hemisphere. PIC/POC ratios in the Southern Ocean are between 0.07 and 0.5, in agreement with observations that this region is strongly dominated by low calcifying Southern Ocean *E. huxleyi* B/C morphotype (Figure 2a; Charalampopoulou et al., 2016; Poulton et al., 2011; Mohan et al., 2008; Findlay and Giraudeau, 2000), which has PIC/POC ratios between 0.1 and 0.3 in culture (Müller et al., 2015).

While simulated coccolithophore PIC/POC ratios match coccolithophore biogeography in most oceanic regions, some areas show a distinct mismatch. For instance model-estimated PIC/POC is greater than the midpoint PIC/POC values shown by corresponding colors in Figure 2a in the western equatorial Pacific and eastern Indian basin. In these areas, the most dominant UPZ coccolithophores are of the uncultured *Umbellosphaera* genus (Figure 2b), within which species are relatively heavily calcified (Young et al., 2014). Lack of representation of *Umbellosphaera* in our physiological data prevents us from precisely evaluating what PIC/POC values should be in these regions. In any case, PIC/POC values for many of the coccolithophore subgroups identified in this study have a large range of environmental plasticity (Figure 1), making evaluation of our modeled coccolithophore PIC/POC using dominant coccolithophore groups challenging.

Nevertheless, our coccolithophore model appears to capture reasonable growth rates and PIC/POC ratios in the surface ocean, compared to what has been observed in culture (Figures 3, 4, and 6 compared to Figure 8). How this will change over the 21st century depends on anthropogenically forced trends in sea surface temperature, CO_2 content, and nutrients. While model results presented in Figure 8 are driven by oceanographic data, we demonstrate that these maps are comparable to those driven by CESM output for the modern day

period (decadal average 2006–2015; Figure S3). Therefore, CESM appears to adequately simulate the present-day coccolithophore environment with respect to pCO_2, PO_4, and temperature at the sea surface. In the following section we use long-term trends in these variables from the CESM-LE to estimate how coccolithophore growth and relative calcification may change by the end of the century.

9.2. Coccolithophore growth and PIC/POC over the 21st century

The CESM-LE forced with RCP 8.5 projects a $2 - 3°C$ increase in SST, approximately a doubling of present day pCO_2, and a $0.1 - 0.4$ μmol L^{-1} decrease in surface PO_4 during the growing season from 2006 to 2100 (Figure 9a–f). Increases in temperature cause increases in growth rate throughout the ocean, with the strongest effects being seen at high latitudes (Figure 9g). As the influence of temperature on PIC/POC is limited to colder temperatures (Figure 4), we project that sea surface warming causes coccolithophore PIC/POC to increase by 0.2 to >0.35 at high latitudes (Figure 9h). Changes in pCO_2 have contrasting effects on growth rate and PIC/POC. pCO_2-driven increases in growth rate are as large as 0.2 d^{-1} while PIC/POC decreases almost uniformly by roughly 0.24 due to increases in pCO_2 (Figure 9i and j). Changes in surface PO_4 concentration over the 21st century have opposite effects on coccolithophore growth rate and PIC/POC. While decreases in PO_4 cause growth rates to slow by more than 0.3 d^{-1}, increases in PIC/POC from P-limitation are geographically variable and between 0.02 and 0.2 (Figure 9k and l). Nearly all changes are statistically significant; long-term ensemble mean changes surpassed standard deviation among ensemble members by at least 2 to 1 (stippled area in Figure 9).

In Figure 10 we present results of our coccolithophore model with all effects active, driven by data from the CESM-LE. These results are a culmination of the equations presented in section 8 and illustrated in Figure 7. Changes in coccolithophore growth rate were primarily driven by changes in temperature at the poles, where growth rate increases, and decreases in PO_4 concentra-

tion in the low and mid latitudes, where growth rate decreases. An interplay between warmer temperatures and decreased nutrient availability can alter coccolithophore growth rates differently at different periods of the year (see Figure S4 for regional time-series of coccolithophore growth rates over the course of a year). Increases in growth rates from increases in pCO_2 are widely overridden by decreases in PO_4, except in some high nutrient regions (though this neglects the potential effects of iron limitation; Figure S4). This is consistent with the results from Feng et al. (2016) who found that nutrient (specifically NO_3) declines were the strongest driver of coccolithophore growth rate changes under future conditions. In contrast, changes in pCO_2 have the strongest effect on PIC/POC in coccolithophores, consistent with Müller et al. (2017) who observed decreases in PIC/POC with increasing pCO_2, regardless of nutrient status. In our model results PIC/POC drops in most mid-latitude regions from $\sim$60°N to $\sim$30°S (Figures 10 and S5). In the Arctic Ocean, we project slight increases in PIC/POC driven by a combination of increased PO_4-limitation and warmer sea surface temperatures (though this region is not a prolific region for coccolithophores; Figure 2). In the Southern Ocean, the Atlantic and Indian sectors show slight increases in PIC/POC from warmer temperatures, while Pacific sector coccolithophore PIC/POC decreases slightly from increased pCO_2 (Figures 10 and S5). Similarly to maps showing the individual effects of drivers (Figure 9), most changes are statistically robust (stippled area in Figure 10).

10. Discussion

We demonstrate that while coccolithophore subgroups appear specialized for growth in diverse oceanic biomes and show individual responses to changes in their environment, the overall trends in surface coccolithophore growth and PIC/POC ratios can be reasonably estimated with a generalized coccolithophore model. Projected anthropogenic changes in the surface ocean over the 21st century have contrasting effects on coccolithophore growth rate and calcification. While increases in pCO_2 and temperature stimulate growth, decreases in nutri-

32

ent availability decrease potential growth rates. By the same token, increases in coccolithophore PIC/POC from increased temperature and nutrient limitation modulate negative effects of increasing pCO_2 on PIC/POC. These counteractive effects on coccolithophore calcification could explain why Marañón et al. (2016) found that current coccolithophore calcification was independent of carbonate chemistry in the tropics. However, as the surface ocean continues to change in response to anthropogenic emissions over this century, some effects will exert more influence than others.

Overall, we project a decline in growth rate and relative calcification in most low- and mid-latitude regions by the end of the century. Northern hemisphere high latitudes may experience faster growth rates with increased calcification, while Southern Ocean calcification shows minor calcification changes in either direction (Figure 10). These changes are a culmination of direct (warming and oceanic CO_2 absorption) and indirect (stratification and nutrient limitation) consequences of human driven climate change over the next ∼80 years. However, coccolithophores may respond differently to the most immediate changes to the surface ocean.

Several recent studies have indicated that coccolithophore populations are expanding poleward, as indicated by a temporally resolved compilation of field and satellite observations (Winter et al., 2013). Specifically in the North Atlantic, coccolithophore populations appear to be responding positively to anthropogenic carbon inputs, increasing in abundance in subtropical (1990–2014; Krumhardt et al., 2016) and subpolar/temperate (1965–2010; Rivero-Calle et al., 2015) regions of the North Atlantic. While an increase in dissolved inorganic carbon concentration in the surface ocean was cited as a major contributing factor to coccolithophore increases in these studies, other effects of anthropogenic climate change, such as warmer sea surface temperatures or increased stratification/nutrient limitation (which favors coccolithophores) could also be underlying factors (Winter et al., 2013; Rivero-Calle et al., 2015). Increases in coccolithophore growth rate and PIC/POC are projected by the end of the century in the high latitude regions in our model (though not in the North Atlantic),

33

mostly attributable to increases in sea surface temperature (see Figures 9 and 10).

However, these studies (especially the North Atlantic studies; Rivero-Calle et al., 2015; Krumhardt et al., 2016) found that a major contributor to coc-
colithophore increases is recent anthropogenic carbon inputs. While long-term projections predict that PO_4 will become increasingly scarce in the North At-lantic and have negative effects on coccolithophore growth rates (unless coc-colithophores can take advantage of organic P sources; Poulton et al., 2017), this PO_4 decrease has not yet been observed, unlike the increases in anthro-
pogenic carbon, which have been well documented (Bates et al., 2014; Sabine et al., 2004). Therefore, while the indirect effect of decreased nutrient availabil-ity from anthropogenic warming-induced stratification has yet to be realized, coccolithophores could be experiencing an alleviation of carbon limitation and perhaps a stimulation in growth from increasing surface pCO_2 and/or warming
surface temperatures.

We tested the possibility of carbon-induced growth rate increases with model simulations parameterized specifically for a *E. huxleyi* morphotype A from the North Atlantic, strain PML B92/11. Specifically, we used the low K_{PO4} reported in Perrin et al. (2016) of 0.051 μM for this morphotype (strain PML B92/11; Table 2) and a K_{CO2} of 270 μatm derived from POC-based growth rates from
Sett et al. (2014) (cultures grown at 20°C; also for strain PML B92/11; data plotted in Figure S2c). We ran our model with these parameterizations on a monthly timestep with time-varying (1982–2011) pCO_2 from Landschützer et al. (2015) and monthly climatologies of PO_4 and sea surface temperature from
World Ocean Database (Boyer et al., 2013). Coccolithophores in the North Atlantic (from subtropics to subpolar) showed 5–10% increases in springtime growth rates over these 30 years with these parameterizations (data not shown), a result consistent with observations shown in Rivero-Calle et al. (2015) and Krumhardt et al. (2016). These effects, however, may be temporary if warming
and stratification cause severe declines in nutrients, as projected by the CESM-LE simulations.

34

Our model also projects decreases in coccolithophore PIC/POC over the 21st century in the Pacific sector of the Southern Ocean with no change or minor increases in the Atlantic and Indian sectors. These decreases are consistent with the satellite record (1998–2014) showing that calcification has decreased in large portions of the Southern Ocean (Freeman and Lovenduski, 2015). The observed decrease over these 17 years could be due to shifts in coccolithophore subgroups (e.g., to the low calcifying Southern Ocean *E. huxleyi* morphotype B/C; Cubillos et al., 2007) or to physiological changes induced by changing carbonate chemistry (Freeman and Lovenduski, 2015) or both – Cubillos et al. (2007) found that the shift between *E. huxleyi* morphotypes A and B/C (Southern Ocean type) followed changes in carbonate chemistry. Indeed, calcification in the low calcifying Southern Ocean morphotype is especially sensitive to increases in pCO_2, increasingly present in a non-calcified, "naked" form under high CO_2 conditions (Müller et al., 2015). Furthermore, considering multiple stressors, Feng et al. (2016) found that increasing pCO_2 is the strongest driver for physiological changes in coccolithophore PIC/POC for an *E. huxleyi* morphotype A strain from the Pacific sector of the Southern Ocean, consistent with our results. Eventually, warmer sea surface temperatures in the Southern Ocean could induce more calcification in *E. huxleyi* or simply select for the higher calcifying morphotype A, as seen in the Atlantic and Indian sectors of the Southern Ocean in our model results (Figure 10). This is important in this Great Calcite Belt region (Balch et al., 2011), as the *E. huxleyi* morphotype constituting a bloom strongly influences overall calcite production (Poulton et al., 2013). In any case, the Southern Ocean *E. huxleyi* morphotype B/C appears to be particularly tolerant of cold, high pCO_2 conditions. Further, calcification does not seem to be crucial for survival and reproduction in this *E. huxleyi* morphotype (Müller et al., 2015). This begs the question of whether decreases in relative calcification, as projected by our model in most oceanic regions (Figure 10), will be a negative feedback to coccolithophore growth resulting in decreased fitness.

Whether decreases in coccolithophore PIC/POC will cause decreases in fitness ultimately depends on the function of the coccoliths, which likely vary

35

between coccolithophore subgroups (Monteiro et al., 2016). Some species (e.g., bloom forming *E. huxleyi*) may synthesize coccoliths to protect from UV damage and excess light (Xu et al., 2016), while others may use coccoliths to capture and channel sparse light in the deep euphotic zone more effectively (e.g., *F. profunda*; Monteiro et al., 2016). Still, others may synthesize coccoliths for protection from grazers, such as spine-bearing coccolithophores (see images in, e.g., Young et al., 2003). In other cases calcification may be a vestigial trait – decreases in calcification may not influence fitness. Monteiro et al. (2016) suggest a diversity of purposes behind extant coccolithophore calcification (grazing protection, viral/bacterial infection protection, high-light protection, and light uptake), but speculate that grazing protection was the original reason coccolithophores evolved calcification. Nevertheless, other phytoplankton competitors, as well as zooplankton grazers, are also subject to adverse (or positive) consequences of anthropogenic climate change. How coccolithophores ultimately fare in an ecological context will be influenced by the ecological fitness of other members of the ecosystem.

Although our work focused on bottom up influences of environmental change on coccolithophore growth and relative calcification, equally important are top down influences in determining the overall success of coccolithophores in a future ocean. This would be ideally studied in mesocosm experiments in a natural context (e.g., Riebesell et al., 2017), as well as in Earth system models with well-developed ecosystem models. Parameterizing coccolithophores as an explicit phytoplankton functional type (PFT) is imperative for predicting their response to environmental change and coincident effects on the global carbon cycle, especially given that coccolithophores are one of major producers of pelagic $CaCO_3$, which is critical for ballasting carbon to the deep sea. However, computing costs limit the complexity of ecosystem models, such that modeling centers are inclined to represent all coccolithophores as a single PFT. Thus, overarching trends across coccolithophore species/morphotypes must be identified, as we have aimed to do here, despite inter-specific variability (see, e.g., Figure 3).

Though we are able to produce reasonable relationships for relating coc-

colithophore growth and calcification to environmental change, several open

¹⁰¹⁰ questions remain. For instance, we have little or no physiological data on certain coccolithophore species, such as those from the *Umbellosphaera* genus or *F. profunda*, which are major components of the coccolithophore community in vast oceanic regions (Figure 2). These species may have alternative nutritional strategies, such as mixotrophy, and may not be obligate phototrophs, a possible

¹⁰¹⁵ reason why they are difficult to isolate and culture under laboratory conditions (Poulton et al., 2017). The *Umbellospharea* genus, specifically, tends to dominate nutrient-deplete surface waters (Haidar and Thierstein, 2001; Okada and Honjo, 1973; Poulton et al., 2017), which could become more prevalent in the future. Incorporating physiological data on these coccolithophore species could

¹⁰²⁰ influence our general relationships for growth rate and calcification under changing environmental conditions. Also, the designation of *E. huxleyi* morphotypes needs better defined boundaries based on genetic, morphological, and physiological data (Read et al., 2013). *E. huxleyi* morphotypes A over-calcified and R closely resemble each other morphologically, inhabit the same latitudinal band

¹⁰²⁵ in the Southern Ocean, and show similar reactions to increased CO_2. Thus, we have grouped them together in this study. On what basis are these two morphotypes really distinct? Having a general over-calcified *E. huxleyi* morphotype would give more weight to the numerous experiments done on *E. huxleyi* morphotype R (since otherwise its observed distribution appears rather limited).

¹⁰³⁰ In addition to physiological testing on the most widespread coccolithophores, an increased understanding of physiological effects of nutrient limitation is necessary. For example, we lack an understanding of how iron limitation affects calcification in coccolithophores. Does iron limitation also induce increased calcification, as does PO_4 limitation? Further, one of the limitations of this study

¹⁰³⁵ is that we represented nutrient changes with changes in PO_4, but a recent study showed NO_3 to be an important factor in determining overall coccolithophore growth (Feng et al., 2016). This is likely due to inefficient NO_3 uptake kinetics in some coccolithophore species/morphotypes (see large K_{NO3} value from Feng et al. (2016) in Table 2). However, coccolithophores can bloom under condi-

tions of low N:P, which are suggestive of superior competitive ability under N limitation (Lessard et al., 2005). Additionally, the usage of organic nutrient sources by coccolithophores increases their ability to thrive where inorganic nutrients are limiting (Benner and Passow, 2010; Poulton et al., 2017); this is not considered here. In any case, further research on relative efficiencies of nutrient uptake by coccolithophores as compared to other phytoplankton will aid in the development and accuracy of marine phytoplankton simulation in Earth system models. An explicit PFT describing coccolithophores will allow more realistic estimates of coccolithophore growth and calcification by simulating competition for nutrients among phytoplankton assemblages and biogeochemical feedbacks resulting from changes in coccolithophore growth and calcification.

11. Conclusions

In this study, we developed an empirical coccolithophore model based on a wide compilation of studies. Our model estimates of coccolithophore growth rate and relative calcification were based on physiological relationships for temperature, PO_4 concentration, and pCO_2. Parameterizations were further guided by current coccolithophore biogeography. By applying this coccolithophore model to output from the CESM-LE and simulating long-term changes in the surface ocean over the 21st century, we demonstrated the potential for our coccolithophore model to be applied in Earth system modeling. Our results showed that changes in coccolithphore growth rates and calcification change by the end of the century vary regionally, highlighting how multiple simultaneous changes in the marine environment modulate biological responses.

This study complements multi-stressor culturing studies, but goes a step further by encompassing all coccolithophore species into one coccolithophore phytoplankton functional type using overarching, across-species relationships. This work highlights important gaps in our understanding of coccolithophore responses to future change, such as understanding how light and iron limitation may affect coccolithophore calcification. Additionally, physiological data

on several major, yet-uncultured coccolithophore species is necessary. The coc-
colithophore model presented here, however, fits our current understanding of
generalized coccolithophore environmental selection across coccolithophore sub-
groups and physiological responses spanning environmental gradients.

12. Acknowledgements

13. References

Andruleit, H., Stäger, S., Rogalla, U., Čepek, P., 2003. Living coccolithophores
in the northern Arabian Sea: ecological tolerances and environmental control.
Marine Micropaleontology 49, 157 – 181. URL: http://www.sciencedirect.
com/science/article/pii/S0377839803000495, doi:http://dx.doi.org/
10.1016/S0377-8398(03)00049-5.

Bach, L.T., Mackinder, L.C.M., Schulz, K.G., Wheeler, G., Schroeder, D.C.,
Brownlee, C., Riebesell, U., 2013. Dissecting the impact of CO_2 and pH
on the mechanisms of photosynthesis and calcification in the coccolithophore
Emiliania huxleyi. New Phytologist 199, 121–134. URL: http://dx.doi.
org/10.1111/nph.12225, doi:10.1111/nph.12225.

Bach, L.T., Riebesell, U., Gutowska, M.A., Federwisch, L., Schulz, K.G., 2015.
A unifying concept of coccolithophore sensitivity to changing carbonate chem-
istry embedded in an ecological framework. Progress in Oceanography 135,
125–138. doi:http://dx.doi.org/10.1016/j.pocean.2015.04.012.

Balch, W., Drapeau, D., Bowler, B., Booth, E., 2007. Prediction of pelagic calcification rates using satellite measurements. Deep Sea Research Part II: Topical Studies in Oceanography 54, 478 – 495. URL: http://www.sciencedirect.com/science/article/pii/S096706450700032X, doi:http://dx.doi.org/10.1016/j.dsr2.2006.12.006. the Role of Marine Organic Carbon and Calcite Fluxes in Driving Global Climate Change, Past and Future.

Balch, W., Gordon, H.R., Bowler, B., Drapeau, D., Booth, E., 2005. Calcium carbonate measurements in the surface global ocean based on Moderate-Resolution Imaging Spectroradiometer data. Journal of Geophysical Research: Oceans 110, 1978–2012.

Balch, W.M., Bates, N.R., Lam, P.J., Twining, B.S., Rosengard, S.Z., Bowler, B.C., Drapeau, D.T., Garley, R., Lubelczyk, L.C., Mitchell, C., Rauschenberg, S., 2016. Factors regulating the great calcite belt in the southern ocean and its biogeochemical significance. Global Biogeochemical Cycles 30, 1124–1144. URL: http://dx.doi.org/10.1002/2016GB005414, doi:10.1002/2016GB005414. 2016GB005414.

Balch, W.M., Drapeau, D.T., Bowler, B.C., Lyczskowski, E., Booth, E.S., Alley, D., 2011. The contribution of coccolithophores to the optical and inorganic carbon budgets during the southern ocean gas exchange experiment: New evidence in support of the "great calcite belt" hypothesis. Journal of Geophysical Research: Oceans 116, n/a–n/a. URL: http://dx.doi.org/10.1029/2011JC006941, doi:10.1029/2011JC006941. c00F06.

Balch, W.M., Holligan, P.M., Kilpatrick, K.A., 1992. Calcification, photosynthesis and growth of the bloom-forming coccolithophore, Emiliania huxleyi. Continental Shelf Research 12, 1353–1374. doi:http://dx.doi.org/10.1016/0278-4343(92)90059-S.

Balestra, B., Ziveri, P., Monechi, S., Troelstra, S., 2004. Coccolithophorids from the Southeast Greenland Margin (northern North Atlantic): production, ecology and the surface sediment record. Micropaleontology 50, 23–

34. URL: http://micropal.geoscienceworld.org/content/50/Suppl_1/ 23, doi:10.2113/50.Suppl_1.23.

Bates, N.R., Asto, Y., Church, M., Currie, K., Dore, J., González-Dávila, M., Lorenzoni, L., Muller-Karger, F., Olafsson, J., Santana-Casiano, J., 2014. A time-series view of changing ocean chemistry due to ocean uptake of anthropogenic CO_2 and ocean acidification. Oceanography 27, 126–141.

Baumann, K.H., Böckel, B., Frenz, M., 2004. Coccolith contribution to South Atlantic carbonate sedimentation. Springer Berlin Heidelberg, Berlin, Heidelberg. pp. 367–402. URL: https://doi.org/10.1007/978-3-662-06278-4_14, doi:10.1007/978-3-662-06278-4_14.

Beaufort, L., Probert, I., de Garidel-Thoron, T., Bendif, E.M., Ruiz-Pino, D., Metzl, N., Goyet, C., Buchet, N., Coupel, P., Grelaud, M., Rost, B., Rickaby, R.E.M., de Vargas, C., 2011. Sensitivity of coccolithophores to carbonate chemistry and ocean acidification. Nature 476, 80–83. URL: http://dx. doi.org/10.1038/nature10295.

Belkin, I.M., Gordon, A.L., 1996. Southern ocean fronts from the greenwich meridian to tasmania. Journal of Geophysical Research: Oceans 101, 3675–3696. URL: http://dx.doi.org/10.1029/95JC02750, doi:10.1029/ 95JC02750.

Benner, I., Passow, U., 2010. Utilization of organic nutrients by coccolithophores. Marine Ecology Progress Series 404, 21–29. URL: http://www. int-res.com/abstracts/meps/v404/p21-29/.

Blanco-Ameijeiras, S., Lebrato, M., Stoll, H.M., Iglesias-Rodriguez, D., Müller, M.N., Méndez-Vicente, A., Oschlies, A., 2016. Phenotypic variability in the coccolithophore Emiliania huxleyi. PLOS ONE 11, 1–17. URL: http: //dx.doi.org/10.1371%2Fjournal.pone.0157697, doi:10.1371/journal. pone.0157697.

41

van Bleijswijk, J., van der Wal, P., Kempers, R., Veldhuis, M., Young, J.R., Muyzer, G., de Vrind-de Jong, E., Westbroek, P., 1991. Distribution of two types of Emiliania huxleyi (Prymnesiophyceae) in the northeast Atlantic region as determined by immunofluorescence and coccolith morphology.

Journal of Phycology 27, 566–570. URL: `http://dx.doi.org/10.1111/j.0022-3646.1991.00566.x`, doi:10.1111/j.0022-3646.1991.00566.x.

van Bleijswijk, J.D.L., Kempers, R.S., Veldhuis, M.J., Westbroek, P., 1994. Cell and growth characteristics of types a and b of Emiliania huxleyi (Prymnesiophyceae) as determined by flow cytometry and chemical analyses. Journal of

Phycology 30, 230–241. URL: `http://dx.doi.org/10.1111/j.0022-3646.1994.00230.x`, doi:10.1111/j.0022-3646.1994.00230.x.

Bolton, C.T., Stoll, H.M., 2013. Late Miocene threshold response of marine algae to carbon dioxide limitation. Nature 500, 558–562. URL: `http://dx.doi.org/10.1038/nature12448`.

Boyd, P.W., Doney, S.C., Strzepek, R., Dusenberry, J., Lindsay, K., Fung, I., 2008. Climate-mediated changes to mixed-layer properties in the Southern Ocean: assessing the phytoplankton response. Biogeosciences 5, 847–864. URL: `https://www.biogeosciences.net/5/847/2008/`, doi:10.5194/bg-5-847-2008.

Boyd, P.W., Rynearson, T.A., Armstrong, E.A., Fu, F., Hayashi, K., Hu, Z., Hutchins, D.A., Kudela, R.M., Litchman, E., Mulholland, M.R., Passow, U., Strzepek, R.F., Whittaker, K.A., Yu, E., Thomas, M.K., 2013. Marine phytoplankton temperature versus growth responses from polar to tropical waters – outcome of a scientific community-wide study. PLOS

ONE 8, 1–17. URL: `https://doi.org/10.1371/journal.pone.0063091`, doi:10.1371/journal.pone.0063091.

Boyer, T., Antonov, J., Baranova, O., Coleman, C., Garcia, H., Grodsky, A., Johnson, D., Locarnini, R., Mishonov, A., O'Brien, T., Paver, C., Reagan,

J., Seidov, D., Smolyar, I., Zweng, M., 2013. World Ocean Database 2013.
₁₁₈₀ volume 72. NOAA Atlas NESDIS. doi:10.7289/V5NZ85MT.

Broecker, W., Clark, E., 2009. Ratio of coccolith $CaCO_3$ to foraminifera
$CaCO_3$ in late Holocene deep sea sediments. Paleoceanography 24, n/a–
n/a. URL: http://dx.doi.org/10.1029/2009PA001731, doi:10.1029/
2009PA001731. pA3205.

₁₁₈₅ Buitenhuis, E.T., De Baar, H.J.W., Veldhuis, M.J.W., 1999. Photosyn-
thesis and calcification by Emiliania huxleyi (Prymnesiophyceae) as a
function of inorganic carbon species. Journal of Phycology 35, 949–
959. URL: http://dx.doi.org/10.1046/j.1529-8817.1999.3550949.x,
doi:10.1046/j.1529-8817.1999.3550949.x.

₁₁₉₀ Buitenhuis, E.T., Geider, R.J., 2010. A model of phytoplankton acclima-
tion to iron–light colimitation. Limnology and Oceanography 55, 714–724.
URL: http://dx.doi.org/10.4319/lo.2010.55.2.0714, doi:10.4319/lo.
2010.55.2.0714.

Buitenhuis, E.T., Hashioka, T., Quéré, C.L., 2013a. Combined constraints on
₁₁₉₅ global ocean primary production using observations and models. Global Bio-
geochemical Cycles 27, 847–858. URL: http://dx.doi.org/10.1002/gbc.
20074, doi:10.1002/gbc.20074.

Buitenhuis, E.T., Pangerc, T., Franklin, D.J., Le Quéré, C., Malin, G., 2008.
Growth rates of six coccolithophorid strains as a function of temperature.
₁₂₀₀ Limnology and Oceanography 53, 1181–1185. URL: http://dx.doi.org/
10.4319/lo.2008.53.3.1181, doi:10.4319/lo.2008.53.3.1181.

Buitenhuis, E.T., Vogt, M., Moriarty, R., Bednaršek, N., Doney, S.C., Leblanc,
K., Le Quéré, C., Luo, Y.W., O'Brien, C., O'Brien, T., Peloquin, J., Schiebel,
R., Swan, C., 2013b. MAREDAT: towards a world atlas of MARine ecosys-
₁₂₀₅ tem DATa. Earth System Science Data 5, 227–239. URL: http://www.
earth-syst-sci-data.net/5/227/2013/, doi:10.5194/essd-5-227-2013.

Cabré, A., Marinov, I., Leung, S., 2015. Consistent global responses of marine ecosystems to future climate change across the IPCC AR5 earth system models. Climate Dynamics 45, 1253–1280. URL: `http://dx.doi.org/10.1007/s00382-014-2374-3`, doi:`10.1007/s00382-014-2374-3`.

Cermeño, P., Lee, J., Wyman, K., Schofield, O., Falkowski, P., 2011. Competitive dynamics in two species of marine phytoplankton under non-equilibrium conditions. Marine Ecology Progress Series 429, 19–28. URL: `http://www.int-res.com/abstracts/meps/v429/p19-28/`.

Charalampopoulou, A., Poulton, A., Tyrrell, T., Lucas, M., 2011. Irradiance and pH affect coccolithophore community composition on a transect between the North Sea and the Arctic Ocean. Marine Ecology Progress Series 431, 25–43. URL: `http://www.int-res.com/abstracts/meps/v431/p25-43/`.

Charalampopoulou, A., Poulton, A.J., Bakker, D.C.E., Lucas, M.I., Stinchcombe, M.C., Tyrrell, T., 2016. Environmental drivers of coccolithophore abundance and calcification across Drake Passage (Southern Ocean). Biogeosciences 2016, 5917–5935. URL: `http://www.biogeosciences.net/13/5917/2016/bg-13-5917-2016.pdf`, doi:`10.5194/bg-13-5917-2016`.

Cook, S.S., Jones, R.C., Vaillancourt, R.E., Hallegraeff, G.M., 2013. Genetic differentiation among Australian and Southern Ocean populations of the ubiquitous coccolithophore Emiliania huxleyi (Haptophyta). Phycologia 52, 368–374. URL: `http://dx.doi.org/10.2216/12-111.1`, doi:`10.2216/12-111.1`, arXiv:`http://dx.doi.org/10.2216/12-111.1`.

Cook, S.S., Whittock, L., Wright, S.W., Hallegraeff, G.M., 2011. Photosynthetic pigment and genetic differences between two southern ocean morphotypes of Emiliania huxleyi (Haptophyta). Journal of Phycology 47, 615–626. URL: `http://dx.doi.org/10.1111/j.1529-8817.2011.00992.x`, doi:`10.1111/j.1529-8817.2011.00992.x`.

Cortés, M.Y., Bollmann, J., Thierstein, H.R., 2001. Coccolithophore ecology at

the HOT station ALOHA, Hawaii. Deep sea research Part II: Topical studies in oceanography 48, 1957–1981.

Cubillos, J., Wright, S., Nash, G., de Salas, M., Griffiths, B., Tilbrook, B., Poisson, A., Hallegraeff, G., 2007. Calcification morphotypes of the coccolithophorid Emiliania huxleyi in the Southern Ocean: changes in 2001 to 2006 compared to historical data. Marine Ecology Progress Series 348, 47–54. URL: `http://www.int-res.com/abstracts/meps/v348/p47-54/`.

Daniels, C.J., Poulton, A.J., Young, J.R., Esposito, M., Humphreys, M.P., Ribas-Ribas, M., Tynan, E., Tyrrell, T., 2016. Species-specific calcite production reveals Coccolithus pelagicus as the key calcifier in the Arctic Ocean. Marine Ecology Progress Series 555, 29–47. URL: `http://www.int-res.com/abstracts/meps/v555/p29-47/`.

Daniels, C.J., Sheward, R.M., Poulton, A.J., 2014. Biogeochemical implications of comparative growth rates of Emiliania huxleyi and Coccolithus species. Biogeosciences 11, 6915–6925. URL: `http://www.biogeosciences.net/11/6915/2014/`, doi:`10.5194/bg-11-6915-2014`.

De Bodt, C., Van Oostende, N., Harlay, J., Sabbe, K., Chou, L., 2010. Individual and interacting effects of pCO_2 and temperature on Emiliania huxleyi calcification: study of the calcite production, the coccolith morphology and the coccosphere size. Biogeosciences 7, 1401–1412. URL: `http://www.biogeosciences.net/7/1401/2010/`, doi:`10.5194/bg-7-1401-2010`.

Diner, R.E., Benner, I., Passow, U., Komada, T., Carpenter, E.J., Stillman, J.H., 2015. Negative effects of ocean acidification on calcification vary within the coccolithophore genus Calcidiscus. Marine Biology 162, 1287–1305. URL: `http://dx.doi.org/10.1007/s00227-015-2669-x`, doi:`10.1007/s00227-015-2669-x`.

Dylmer, C., Giraudeau, J., Hanquiez, V., Husum, K., 2015. The coccolithophores Emiliania huxleyi and Coccolithus pelagicus: Extant populations from the Norwegian–Iceland seas and Fram Strait.

Deep Sea Research Part I: Oceanographic Research Papers 98, 1 – 9. URL: http://www.sciencedirect.com/science/article/pii/S0967063714002271, doi:http://doi.org/10.1016/j.dsr.2014.11.012.

Emerson, S., Hedges, J., 2008. Chemical oceanography and the marine carbon cycle. Cambridge University Press.

Eppley, R.W., Rogers, J.N., McCarthy, J.J., 1969. Half-saturation constants for uptake of nitrate and ammonium by marine phytoplankton. Limnology and Oceanography 14, 912–920. URL: http://dx.doi.org/10.4319/lo.1969.14.6.0912, doi:10.4319/lo.1969.14.6.0912.

Feng, Y., Roleda, M.Y., Armstrong, E., Boyd, P.W., Hurd, C.L., 2016. Environmental controls on the growth, photosynthetic and calcification rates of a Southern Hemisphere strain of the coccolithophore Emiliania huxleyi. Limnology and Oceanography , n/a–n/aURL: http://dx.doi.org/10.1002/lno.10442, doi:10.1002/lno.10442.

Feng, Y., Warner, M.E., Zhang, Y., Sun, J., Fu, F.X., Rose, J.M., Hutchins, D.A., 2008. Interactive effects of increased pCO_2, temperature and irradiance on the marine coccolithophore Emiliania huxleyi (Prymnesiophyceae). European Journal of Phycology 43, 87–98. URL: http://dx.doi.org/10.1080/09670260701664674, doi:10.1080/09670260701664674, arXiv:http://dx.doi.org/10.1080/09670260701664674.

Fielding, S.R., 2013. Emiliania huxleyi specific growth rate dependence on temperature. Limnology and Oceanography 58, 663–666. URL: http://dx.doi.org/10.4319/lo.2013.58.2.0663, doi:10.4319/lo.2013.58.2.0663.

Findlay, C., Giraudeau, J., 2000. Extant calcareous nannoplankton in the Australian sector of the Southern Ocean (Austral summers 1994 and 1995). Marine Micropaleontology 40, 417 – 439. URL: http://www.sciencedirect.com/science/article/pii/S0377839800000463, doi:http://dx.doi.org/10.1016/S0377-8398(00)00046-3.

Findlay, H.S., Calosi, P., Crawfurd, K., 2011. Determinants of the PIC:POC response in the coccolithophore Emiliania huxleyi under future ocean acidification scenarios. Limnology and Oceanography 56, 1168–1178. URL: http://dx.doi.org/10.4319/lo.2011.56.3.1168, doi:10.4319/lo.2011.56.3.1168.

Fiorini, S., Middelburg, J., Gattuso, J., 2011. Effects of elevated CO_2 partial pressure and temperature on the coccolithophore Syracosphaera pulchra. Aquatic Microbial Ecology 64, 221–232. URL: http://www.int-res.com/abstracts/ame/v64/n3/p221-232/.

Flynn, K.J., Clark, D.R., Wheeler, G., 2016. The role of coccolithophore calcification in bioengineering their environment. Proceedings of the Royal Society of London B: Biological Sciences 283. URL: http://rspb.royalsocietypublishing.org/content/283/1833/20161099, doi:10.1098/rspb.2016.1099, arXiv:http://rspb.royalsocietypublishing.org/content/283/1833/20161099.full.pdf.

Freeman, N.M., Lovenduski, N.S., 2015. Decreased calcification in the Southern Ocean over the satellite record. Geophysical Research Letters 42, 1834–1840. URL: http://dx.doi.org/10.1002/2014GL062769, doi:10.1002/2014GL062769.

Freeman, N.M., Lovenduski, N.S., 2016. Mapping the Antarctic Polar Front: Weekly realizations from 2002 to 2014, links to NetCDF file and MPEG4 movie. URL: https://doi.org/10.1594/PANGAEA.855640, doi:10.1594/PANGAEA.855640. supplement to: Freeman, NM; Lovenduski, NS (2016): Mapping the Antarctic Polar Front: weekly realizations from 2002 to 2014. Earth System Science Data, 8(1), 191-198, https://doi.org/10.5194/essd-8-191-2016.

Gerecht, A.C., Šupraha, L., Edvardsen, B., Probert, I., Henderiks, J., 2014. High temperature decreases the PIC/POC ratio and increases phosphorus requirements in Coccolithus pelagicus (Haptophyta). Biogeosciences

11, 3531–3545. URL: http://www.biogeosciences.net/11/3531/2014/, doi:10.5194/bg-11-3531-2014.

Gordon, H.R., Boynton, G.C., Balch, W.M., Groom, S.B., Harbour, D.S., Smyth, T.J., 2001. Retrieval of coccolithophore calcite concentration from ₁₃₂₅ SeaWiFS imagery. Geophysical Research Letters 28, 1587–1590. URL: http://dx.doi.org/10.1029/2000GL012025, doi:10.1029/2000GL012025.

Gregg, W.W., Casey, N.W., 2007. Modeling coccolithophores in the global oceans. Deep Sea Research Part II: Topical Studies in Oceanography 54, 447 – 477. URL: http://www.sciencedirect.com/science/article/ ₁₃₃₀ pii/S0967064507000318, doi:http://dx.doi.org/10.1016/j.dsr2.2006. 12.007. the Role of Marine Organic Carbon and Calcite Fluxes in Driving Global Climate Change, Past and Future.

Gruber, N., 2011. Warming up, turning sour, losing breath: ocean biogeochemistry under global change. Philosophical Transactions of the Royal So-₁₃₃₅ ciety of London A: Mathematical, Physical and Engineering Sciences 369, 1980–1996. URL: http://rsta.royalsocietypublishing.org/content/ 369/1943/1980.abstract.

Guptha, M.V.S., Mergulhao, L.P., Murty, V.S.N., Shenoy, D.M., 2005. Living coccolithophores during the northeast monsoon from the Equatorial Indian ₁₃₄₀ Ocean: Implications on hydrography. Deep Sea Research Part II: Topical Studies in Oceanography 52, 2048–2060. URL: http://www.sciencedirect. com/science/article/pii/S0967064505001347, doi:http://dx.doi.org/ 10.1016/j.dsr2.2005.05.010.

Hagino, K., Bendif, E.M., Young, J.R., Kogame, K., Probert, I., Takano, Y., ₁₃₄₅ Horiguchi, T., de Vargas, C., Okada, H., 2011. New evidence for morphological and genetic variation in the cosmopolitan coccolithophore Emiliania huxleyi (Prymnesiophyceae) from the cox1b-atp4 genes. Journal of Phycology 47, 1164–1176. URL: http://dx.doi.org/10.1111/j.1529-8817.2011.01053. x, doi:10.1111/j.1529-8817.2011.01053.x.

Hagino, K., Okada, H., 2004. Floral response of coccolithophores to progressive oligotrophication in the South Equatorial Current, Pacific Ocean. Global Enivronmental Change in the Ocean and on Land , 121–132.

Hagino, K., Okada, H., Matsuoka, H., 2000. Spatial dynamics of coccolithophore assemblages in the Equatorial Western-Central Pacific Ocean. Marine Micropaleontology 39, 53 – 72. URL: http://www.sciencedirect.com/science/article/pii/S0377839800000141, doi:http://dx.doi.org/10.1016/S0377-8398(00)00014-1.

Hagino, K., Okada, H., Matsuoka, H., 2005. Coccolithophore assemblages and morphotypes of Emiliania huxleyi in the boundary zone between the cold Oyashio and warm Kuroshio currents off the coast of Japan. Marine Micropaleontology 55, 19 – 47. URL: http://www.sciencedirect.com/science/article/pii/S0377839805000149, doi:http://dx.doi.org/10.1016/j.marmicro.2005.02.002.

Haidar, A.T., Thierstein, H.R., 2001. Coccolithophore dynamics of Bermuda (N. Atlantic). Deep Sea Research Part II: Topical Studies in Oceanography 48, 1925–1956.

Henderiks, J., Winter, A., Elbrächter, M., Feistel, R., van der Plas, A., Nausch, G., Barlow, R., 2012. Environmental controls on Emiliania huxleyi morphotypes in the Benguela coastal upwelling system (SE Atlantic). Marine Ecology Progress Series 448, 51–66. URL: http://www.int-res.com/abstracts/meps/v448/p51-66/.

Hense, I., Stemmler, I., Sonntag, S., 2017. Ideas and perspectives: climate-relevant marine biologically driven mechanisms in Earth system models. Biogeosciences 14, 403–413. URL: http://www.biogeosciences.net/14/403/2017/, doi:10.5194/bg-14-403-2017.

Holligan, P., Charalampopoulou, A., Hutson, R., 2010. Seasonal distributions of the coccolithophore, Emiliania huxleyi, and of particulate inorganic carbon in surface waters of the Scotia Sea. Journal

49

of Marine Systems 82, 195 – 205. URL: http://www.sciencedirect.com/science/article/pii/S0924796310000965, doi:http://dx.doi.org/10.1016/j.jmarsys.2010.05.007.

Iglesias-Rodríguez, M.D., Brown, C.W., Doney, S.C., Kleypas, J., Kolber, D., Kolber, Z., Hayes, P.K., Falkowski, P.G., 2002. Representing key phytoplankton functional groups in ocean carbon cycle models: Coccolithophorids. Global Biogeochemical Cycles 16, 47–1–47–20. URL: http://dx.doi.org/10.1029/2001GB001454, doi:10.1029/2001GB001454. 1100.

Iglesias-Rodriguez, M.D., Halloran, P.R., Rickaby, R.E.M., Hall, I.R., Colmenero-Hidalgo, E., Gittins, J.R., Green, D.R.H., Tyrrell, T., Gibbs, S.J., von Dassow, P., Rehm, E., Armbrust, E.V., Boessenkool, K.P., 2008. Phytoplankton calcification in a high-CO_2 world. Science 320, 336–340. URL: http://www.sciencemag.org/content/320/5874/336.abstract, doi:10.1126/science.1154122, arXiv:http://www.sciencemag.org/content/320/5874/336.full.pdf.

Kay, J.E., Deser, C., Phillips, A., Mai, A., Hannay, C., Strand, G., Arblaster, J.M., Bates, S.C., Danabasoglu, G., Edwards, J., Holland, M., Kushner, P., Lamarque, J.F., Lawrence, D., Lindsay, K., Middleton, A., Munoz, E., Neale, R., Oleson, K., Polvani, L., Vertenstein, M., 2015. The Community Earth System Model (CESM) large ensemble project: A community resource for studying climate change in the presence of internal climate variability. Bulletin of the American Meteorological Society 96, 1333–1349. URL: http://dx.doi.org/10.1175/BAMS-D-13-00255.1, doi:10.1175/BAMS-D-13-00255.1.

Klaas, C., Archer, D.E., 2002. Association of sinking organic matter with various types of mineral ballast in the deep sea: Implications for the rain ratio. Global Biogeochemical Cycles 16, 63–1–63–14. URL: http://dx.doi.org/10.1029/2001GB001765, doi:10.1029/2001GB001765. 1116.

Kottmeier, D.M., Rokitta, S.D., Rost, B., 2016. H^+-driven increase in CO_2 uptake and decrease in HCO_3 uptake explain coccolithophores' acclimation re-

50

sponses to ocean acidification. Limnology and Oceanography , n/a–n/aURL: http://dx.doi.org/10.1002/lno.10352, doi:10.1002/lno.10352.

₁₄₁₀ Krumhardt, K.M., Lovenduski, N.S., Freeman, N.M., Bates, N.R., 2016. Apparent increase in coccolithophore abundance in the subtropical North Atlantic from 1990 to 2014. Biogeosciences 13, 1163–1177. URL: http://www.biogeosciences.net/13/1163/2016/, doi:10.5194/bg-13-1163-2016.

Krumhardt, K.M., Lovenduski, N.S., Long, M.C., Lindsay, K., 2017. Avoid-₁₄₁₅ able impacts of ocean warming on marine primary production: Insights from the CESM ensembles. Global Biogeochemical Cycles 31, 114–133. URL: http://dx.doi.org/10.1002/2016GB005528, doi:10.1002/2016GB005528. 2016GB005528.

Landschützer, P., Gruber, N., Bakker, D., 2015. A 30 year observation-based ₁₄₂₀ global monthly gridded sea surface pCO$_2$ product from 1982 through 2011. Carbon Dioxide Information Analysis Center, Oak Ridge National Laboratory, US Department of Energy, Oak Ridge, Tennessee. URL: http://cdiac.ornl.gov/ftp/oceans/spco2_1982_2011_ETH_SOM-FFN.

Langer, G., Geisen, M., Baumann, K.H., Kläs, J., Riebesell, U., Thoms, ₁₄₂₅ S., Young, J.R., 2006. Species-specific responses of calcifying algae to changing seawater carbonate chemistry. Geochemistry, Geophysics, Geosystems 7. URL: http://dx.doi.org/10.1029/2005GC001227, doi:10.1029/2005GC001227.

Langer, G., Gussone, N., Nehrke, G., Riebesell, U., Eisenhauer, A., Thoms, ₁₄₃₀ S., 2007. Calcium isotope fractionation during coccolith formation in emiliania huxleyi: Independence of growth and calcification rate. Geochemistry, Geophysics, Geosystems 8, n/a–n/a. URL: http://dx.doi.org/10.1029/2006GC001422, doi:10.1029/2006GC001422. q05007.

Langer, G., Nehrke, G., Probert, I., Ly, J., Ziveri, P., 2009. Strain-specific re-₁₄₃₅ sponses of Emiliania huxleyi to changing seawater carbonate chemistry. Bio-

geosciences 6, 2637–2646. URL: http://www.biogeosciences.net/6/2637/2009/, doi:10.5194/bg-6-2637-2009.

Laufkötter, C., Vogt, M., Gruber, N., Aita-Noguchi, M., Aumont, O., Bopp, L., Buitenhuis, E., Doney, S.C., Dunne, J., Hashioka, T., Hauck, J., Hirata, T., John, J., Le Quéré, C., Lima, I.D., Nakano, H., Seferian, R., Totterdell, I., Vichi, M., Völker, C., 2015. Drivers and uncertainties of future global marine primary production in marine ecosystem models. Biogeosciences 12, 6955–6984. URL: http://www.biogeosciences.net/12/6955/2015/, doi:10.5194/bg-12-6955-2015.

Lauvset, S.K., Key, R.M., Olsen, A., van Heuven, S., Velo, A., Lin, X., Schirnick, C., Kozyr, A., Tanhua, T., Hoppema, M., Jutterström, S., Steinfeldt, R., Jeansson, E., Ishii, M., Pérez, F.F., Suzuki, T., Watelet, S., 2016. A new global interior ocean mapped climatology: the $1\,°$x$1\,°$ glodap version 2. Earth System Science Data 8, 325–340. doi:10.5194/essd-8-325-2016.

Le Quéré, C., Harrison, S.P., Colin Prentice, I., Buitenhuis, E.T., Aumont, O., Bopp, L., Claustre, H., Cotrim Da Cunha, L., Geider, R., Giraud, X., Klaas, C., Kohfeld, K.E., Legendre, L., Manizza, M., Platt, T., Rivkin, R.B., Sathyendranath, S., Uitz, J., Watson, A.J., Wolf-Gladrow, D., 2005. Ecosystem dynamics based on plankton functional types for global ocean biogeochemistry models. Global Change Biology 11, 2016–2040. URL: http://dx.doi.org/10.1111/j.1365-2486.2005.1004.x, doi:10.1111/j.1365-2486.2005.1004.x.

Lessard, E.J., Merico, A., Tyrrell, T., 2005. Nitrate : phosphate ratios and Emiliania huxleyi blooms. Limnology and Oceanography 50, 1020–1024. URL: http://dx.doi.org/10.4319/lo.2005.50.3.1020, doi:10.4319/lo.2005.50.3.1020.

Lovenduski, N.S., McKinley, G.A., Fay, A.R., Lindsay, K., Long, M.C., 2016. Partitioning uncertainty in ocean carbon uptake projections: Internal variability, emission scenario, and model structure. Global Biogeochemical Cycles

52

1465 , n/a–n/aURL: http://dx.doi.org/10.1002/2016GB005426, doi:10.1002/2016GB005426. 2016GB005426.

Marañón, E., Balch, W.M., Cermeño, P., González, N., Sobrino, C., Fernández, A., Huete-Ortega, M., López-Sandoval, D.C., Delgado, M., Estrada, M., Álvarez, M., Fernández-Guallart, E., Pelejero, C., 2016. Coccolithophore cal-1470 cification is independent of carbonate chemistry in the tropical ocean. Limnology and Oceanography 61, 1345–1357. URL: http://dx.doi.org/10.1002/lno.10295, doi:10.1002/lno.10295.

Matson, P.G., Ladd, T.M., Halewood, E.R., Sangodkar, R.P., Chmelka, B.F., Iglesias-Rodriguez, M.D., 2016. Intraspecific differences in biogeochemi-1475 cal responses to thermal change in the coccolithophore Emiliania huxleyi. PLOS ONE 11, 1–22. URL: http://dx.doi.org/10.1371%2Fjournal.pone.0162313, doi:10.1371/journal.pone.0162313.

Mohan, R., Mergulhao, L.P., Guptha, M., Rajakumar, A., Thamban, M., AnilKumar, N., Sudhakar, M., Ravindra, R., 2008. Ecology of 1480 coccolithophores in the Indian sector of the Southern Ocean. Marine Micropaleontology 67, 30 – 45. URL: http://www.sciencedirect.com/science/article/pii/S0377839807000904, doi:http://dx.doi.org/10.1016/j.marmicro.2007.08.005.

Monteiro, F.M., Bach, L.T., Brownlee, C., Bown, P., Rickaby, R.E.M., Poul-1485 ton, A.J., Tyrrell, T., Beaufort, L., Dutkiewicz, S., Gibbs, S., Gutowska, M.A., Lee, R., Riebesell, U., Young, J., Ridgwell, A., 2016. Why marine phytoplankton calcify. Science Advances 2. URL: http://advances.sciencemag.org/content/2/7/e1501822, doi:10.1126/sciadv.1501822, arXiv:http://advances.sciencemag.org/content/2/7/e1501822.full.pdf.

1490 Moore, J.K., Doney, S.C., Lindsay, K., 2004. Upper ocean ecosystem dynamics and iron cycling in a global three-dimensional model. Global Biogeochemical Cycles 18. URL: http://dx.doi.org/10.1029/2004GB002220, doi:10.1029/2004GB002220. gB4028.

Müller, M.N., Antia, A.N., LaRoche, J., 2008. Influence of cell cycle phase on calcification in the coccolithophore Emiliania huxleyi. Limnology and Oceanography 53, 506–512. URL: http://dx.doi.org/10.4319/lo.2008.53.2.0506, doi:10.4319/lo.2008.53.2.0506.

Müller, M.N., Trull, T., Hallegraeff, G., 2015. Differing responses of three Southern Ocean Emiliania huxleyi ecotypes to changing seawater carbonate chemistry. Marine Ecology Progress Series 531, 81–90. URL: http://www.int-res.com/abstracts/meps/v531/p81-90/.

Müller, M.N., Trull, T.W., Hallegraeff, G.M., 2017. Independence of nutrient limitation and carbon dioxide impacts on the Southern Ocean coccolithophore Emiliania huxleyi. The ISME Journal .

Nanninga, H., Tyrrell, T., 1996. Importance of light for the formation of algal blooms by Emiliania huxleyi. Marine Ecology Progress Series 136, 195–203. URL: http://www.int-res.com/abstracts/meps/v136/p195-203/.

Nimer, N.A., Merret, M.J., 1992. Calcification and utilization of inorganic carbon by the coccolithophorid Emiliania huxleyi Lohmann. The New Phytologist 121, 173–177.

Nimer, N.A., Merret, M.J., 1993. Calcification rate in Emiliania huxleyi Lohmann in response to light, nitrate and availability of inorganic carbon. New Phytologist 123, 673–677. URL: http://dx.doi.org/10.1111/j.1469-8137.1993.tb03776.x, doi:10.1111/j.1469-8137.1993.tb03776.x.

O'Brien, C.J., Vogt, M., Gruber, N., 2016. Global coccolithophore diversity: Drivers and future change. Progress in Oceanography 140, 27–42. URL: http://www.sciencedirect.com/science/article/pii/S0079661115002128, doi:http://dx.doi.org/10.1016/j.pocean.2015.10.003.

Okada, H., Honjo, S., 1973. The distribution of oceanic coccolithophorids in the pacific. Deep Sea Research and Oceanographic Abstracts 20, 355 – 374. URL: http://www.sciencedirect.com/science/article/

pii/0011747173900594, doi:http://dx.doi.org/10.1016/0011-7471(73)90059-4.

Oviedo, A., Ziveri, P., Álvarez, M., Tanhua, T., 2015. Is coccolithophore dis₁₅₂₅tribution in the Mediterranean Sea related to seawater carbonate chemistry? Ocean Science 11, 13–32. URL: http://www.ocean-sci.net/11/13/2015/, doi:10.5194/os-11-13-2015.

Paasche, E., 1998. Roles of nitrogen and phosphorus in coccolith formation in Emiliania huxleyi (Prymnesiophyceae). European ₁₅₃₀Journal of Phycology 33, 33–42. doi:10.1080/09670269810001736513, arXiv:http://dx.doi.org/10.1080/09670269810001736513.

Paasche, E., 2002. A review of the coccolithophorid Emiliania huxleyi (Prymnesiophyceae), with particular reference to growth, coccolith formation, and calcification-photosynthesis interactions. ₁₅₃₅Phycologia 40, 503–529. URL: http://dx.doi.org/10.2216/i0031-8884-40-6-503.1, doi:10.2216/i0031-8884-40-6-503.1, arXiv:http://dx.doi.org/10.2216/i0031-8884-40-6-503.1.

Paasche, E., Brubak, S., 1994. Enhanced calcification in the coccolithophorid Emiliania huxleyi (Haptophyceae) under phosphorus lim₁₅₄₀itation. Phycologia 33, 324–330. URL: http://dx.doi.org/10.2216/i0031-8884-33-5-324.1, doi:10.2216/i0031-8884-33-5-324.1, arXiv:http://dx.doi.org/10.2216/i0031-8884-33-5-324.1.

Patil, S.M., Mohan, R., Shetye, S., Gazi, S., Jafar, S., 2014. Morphological variability of Emiliania huxleyi in the Indian sector of the Southern Oean ₁₅₄₅during the austral summer of 2010. Marine Micropaleontology 107, 44 – 58. URL: http://www.sciencedirect.com/science/article/pii/S0377839814000085, doi:https://doi.org/10.1016/j.marmicro.2014.01.005.

Perrin, L., Probert, I., Langer, G., Aloisi, G., 2016. Growth of the coccol₁₅₅₀ithophore *Emiliania huxleyi* in light- and nutrient-limited batch reactors: rel-

evance for the BIOSOPE deep ecological niche of coccolithophores. Biogeosciences 13, 5983–6001. URL: http://www.biogeosciences.net/13/5983/2016/, doi:10.5194/bg-13-5983-2016.

Poulton, A., Young, J., Bates, N., Balch, W., 2011. Biometry of detached Emiliania huxleyi coccoliths along the Patagonian Shelf. Marine Ecology Progress Series 443, 1–17. URL: http://www.int-res.com/abstracts/meps/v443/p1-17/.

Poulton, A.J., Adey, T.R., Balch, W.M., Holligan, P.M., 2007. Relating coccolithophore calcification rates to phytoplankton community dynamics: Regional differences and implications for carbon export. Deep Sea Research Part II: Topical Studies in Oceanography 54, 538–557. URL: http://www.sciencedirect.com/science/article/pii/S0967064507000355, doi:http://dx.doi.org/10.1016/j.dsr2.2006.12.003. the Role of Marine Organic Carbon and Calcite Fluxes in Driving Global Climate Change, Past and Future.

Poulton, A.J., Holligan, P.M., Charalampopoulou, A., Adey, T.R., 2017. Coccolithophore ecology in the tropical and subtropical Atlantic Ocean: New perspectives from the Atlantic meridional transect (AMT) programme. Progress in Oceanography URL: http://www.sciencedirect.com/science/article/pii/S0079661116300234, doi:https://doi.org/10.1016/j.pocean.2017.01.003.

Poulton, A.J., Painter, S.C., Young, J.R., Bates, N.R., Bowler, B., Drapeau, D., Lyczsckowski, E., Balch, W.M., 2013. The 2008 Emilania huxleyi bloom along the Patagonian Shelf: Ecology, biogeochemistry, and cellular calcification. Global Biogeochemical Cycles 27, 1023–1033. URL: http://dx.doi.org/10.1002/2013GB004641, doi:10.1002/2013GB004641. 2013GB004641.

Poulton, A.J., Stinchcombe, M.C., Achterberg, E.P., Bakker, D.C.E., Dumousseaud, C., Lawson, H.E., Lee, G.A., Richier, S., Suggett, D.J., Young, J.R., 2014. Coccolithophores on the north-west European shelf:

calcification rates and environmental controls. Biogeosciences 11, 3919–3940. URL: http://www.biogeosciences.net/11/3919/2014/, doi:10.5194/bg-11-3919-2014.

Read, B.A., Kegel, J., Klute, M.J., Kuo, A., Lefebvre, S.C., Maumus, F., Mayer, C., Miller, J., Monier, A., Salamov, A., Young, J., Aguilar, M., Claverie, J.M., Frickenhaus, S., Gonzalez, K., Herman, E.K., Lin, Y.C., Napier, J., Ogata, H., Sarno, A.F., Shmutz, J., Schroeder, D., de Vargas, C., Verret, F., von Dassow, P., Valentin, K., Van de Peer, Y., Wheeler, G., huxleyi Annotation Consortium, E., Dacks, J.B., Delwiche, C.F., Dyhrman, S.T., Glockner, G., John, U., Richards, T., Worden, A.Z., Zhang, X., Grigoriev, I.V., 2013. Pan genome of the phytoplankton Emiliania underpins its global distribution. Nature 499, 209–213. URL: http://dx.doi.org/10.1038/nature12221.

Reinfelder, J.R., 2011. Carbon concentrating mechanisms in eukaryotic marine phytoplankton. Annual Review of Marine Science 3, 291–315.

Rickaby, R.E.M., Henderiks, J., Young, J.N., 2010. Perturbing phytoplankton: response and isotopic fractionation with changing carbonate chemistry in two coccolithophore species. Climate of the Past 6, 771–785. URL: http://www.clim-past.net/6/771/2010/, doi:10.5194/cp-6-771-2010.

Riebesell, U., 2004. Effects of CO_2 enrichment on marine phytoplankton. Journal of Oceanography 60, 719–729. URL: http://dx.doi.org/10.1007/s10872-004-5764-z, doi:10.1007/s10872-004-5764-z.

Riebesell, U., Bach, L.T., Bellerby, R.G.J., Monsalve, J.R.B., Boxhammer, T., Czerny, J., Larsen, A., Ludwig, A., Schulz, K.G., 2017. Competitive fitness of a predominant pelagic calcifier impaired by ocean acidification. Nature Geoscience 10, 19–23. URL: http://dx.doi.org/10.1038/ngeo2854.

Riebesell, U., Zondervan, I., Rost, B., Tortell, P.D., Zeebe, R.E., Morel, F.M.M., 2000. Reduced calcification of marine plankton in response to increased atmospheric CO_2. Nature 407, 364–367. URL: http://dx.doi.org/10.1038/35030078.

Riegman, R., Stolte, W., Noordeloos, A.A.M., Slezak, D., 2000. Nu-

₁₆₁₀   trient uptake and alkaline phosphatase (EC 3:1:3:1) activity of *Emil-iania huxleyi* (PRYMNESIOPHYCEAE) during growth under N and P limitation in continuous cultures. Journal of Phycology 36, 87–96. URL: `http://dx.doi.org/10.1046/j.1529-8817.2000.99023.x`, doi:`10.1046/j.1529-8817.2000.99023.x`.

₁₆₁₅ Rivero-Calle, S., Gnanadesikan, A., Del Castillo, C.E., Balch, W.M., Guikema, S.D., 2015. Multidecadal increase in North Atlantic coccolithophores and the potential role of rising CO_2. Science 350, 1533–1537. URL: `http://science.sciencemag.org/content/350/6267/1533`, doi:`10.1126/science.aaa8026`, arXiv:`http://science.sciencemag.org/content/350/6267/1533.full.pdf`.

₁₆₂₀ Rokitta, S.D., Rost, B., 2012. Effects of CO_2 and their modulation by light in the life-cycle stages of the coccolithophore Emiliania huxleyi. Limnology and Oceanography 57, 607–618. URL: `http://dx.doi.org/10.4319/lo.2012.57.2.0607`, doi:`10.4319/lo.2012.57.2.0607`.

Rosas-Navarro, A., Langer, G., Ziveri, P., 2016. Temperature affects the

₁₆₂₅   morphology and calcification of *Emiliania huxleyi* strains. Biogeosciences 13, 2913–2926. URL: `http://www.biogeosciences.net/13/2913/2016/`, doi:`10.5194/bg-13-2913-2016`.

Rost, B., Riebesell, U., Burkhardt, S., Sültemeyer, D., 2003. Carbon acqui-sition of bloom-forming marine phytoplankton. Limnology and Oceanog-

₁₆₃₀   raphy 48, 55–67. URL: `http://dx.doi.org/10.4319/lo.2003.48.1.0055`, doi:`10.4319/lo.2003.48.1.0055`.

Rouco, M., Branson, O., Lebrato, M., Iglesias-Rodriguez, M.D., 2013. The effect of nitrate and phosphate availability on Emiliania huxleyi (NZEH) physiology under different CO_2 scenarios. Frontiers in Microbiology 4,

₁₆₃₅   155. URL: `http://journal.frontiersin.org/article/10.3389/fmicb.2013.00155`, doi:`10.3389/fmicb.2013.00155`.

Saavedra-Pellitero, M., Flores, J.A., Baumann, K.H., Sierro, F.J., 2010. Coccolith distribution patterns in surface sediments of Equatorial and Southeastern Pacific Ocean. Geobios 43, 131 – 149. URL: http://www.sciencedirect.com/science/article/pii/S0016699509000977, doi:http://dx.doi.org/10.1016/j.geobios.2009.09.004. 12th Meeting of the International Nannoplankton Association, Lyon 2008.

Sabine, C.L., Feely, R.A., Gruber, N., Key, R.M., Lee, K., Bullister, J.L., Wanninkhof, R., Wong, C.S., Wallace, D.W.R., Tilbrook, B., Millero, F.J., Peng, T.H., Kozyr, A., Ono, T., Rios, A.F., 2004. The oceanic sink for anthropogenic CO_2. Science 305, 367–371. URL: http://www.sciencemag.org/content/305/5682/367.abstract, doi:10.1126/science.1097403, arXiv:http://www.sciencemag.org/content/305/5682/367.full.pdf.

Sarmiento, J.L., Gruber, N., 2006. Ocean Biogeochemical Dynamics. Princeton University Press.

Saruwatari, K., Satoh, M., Harada, N., Suzuki, I., Shiraiwa, Y., 2016. Change in coccolith size and morphology due to response to temperature and salinity in coccolithophore *Emiliania huxleyi* (Haptophyta) isolated from the Bering and Chukchi seas. Biogeosciences 13, 2743–2755. URL: http://www.biogeosciences.net/13/2743/2016/, doi:10.5194/bg-13-2743-2016.

Schiebel, R., 2002. Planktic foraminiferal sedimentation and the marine calcite budget. Global Biogeochemical Cycles 16, 3–1–3–21. URL: http://dx.doi.org/10.1029/2001GB001459, doi:10.1029/2001GB001459. 1065.

Sett, S., Bach, L.T., Schulz, K.G., Koch-Klavsen, S., Lebrato, M., Riebesell, U., 2014. Temperature modulates coccolithophorid sensitivity of growth, photosynthesis and calcification to increasing seawater pCO_2. PLoS ONE 9, e88308. URL: http://dx.doi.org/10.1371%2Fjournal.pone.0088308, doi:10.1371/journal.pone.0088308.

Sheward, R.M., Poulton, A.J., Gibbs, S.J., Daniels, C.J., Bown, P.R.,

2017. Physiology regulates the relationship between coccosphere geometry and growth phase in coccolithophores. Biogeosciences 14, 1493–1509. URL: https://www.biogeosciences.net/14/1493/2017/, doi:10.5194/bg-14-1493-2017.

Sunda, W.G., Huntsman, S.A., 1995. Iron uptake and growth limitation in oceanic and coastal phytoplankton. Marine Chemistry 50, 189–206. doi:10.1016/0304-4203(95)00035-P.

Taylor, A.R., Brownlee, C., Wheeler, G., 2017. Coccolithophore cell biology: Chalking up progress. Annual Review of Marine Science 9, 283–310. doi:10.1146/annurev-marine-122414-034032.

Tsutsui, H., Takahashi, K., Asahi, H., Jordan, R.W., Nishida, S., Nishiwaki, N., Yamamoto, S., 2016. Nineteen-year time-series sediment trap study of Coccolithus pelagicus and Emiliania huxleyi (calcareous nannoplankton) fluxes in the Bering Sea and subarctic Pacific Ocean. Deep Sea Research Part II: Topical Studies in Oceanography 125–126, 227 – 239. URL: http://www.sciencedirect.com/science/article/pii/S0967064516300145, doi:http://dx.doi.org/10.1016/j.dsr2.2016.02.005. plio-Pleistocene Paleoceanography of the Bering Sea.

Tyrrell, T., Taylor, A., 1996. A modelling study of Emiliania huxleyi in the NE Atlantic. Journal of Marine Systems 9, 83–112.

Watabe, N., Wilbur, K.M., 1966. Effects of temperature on growth, calcification, and coccolith form in Coccolithus huxleyi (Coccolithineae). Limnology and Oceanography 11, 567–575. URL: http://dx.doi.org/10.4319/lo.1966.11.4.0567, doi:10.4319/lo.1966.11.4.0567.

Winter, A., 1985. Distribution of living coccolithophores in the California Current system, southern California borderland. Marine Micropaleontology 9, 385 – 393. URL: http://www.sciencedirect.com/science/article/pii/0377839885900076, doi:http://dx.doi.org/10.1016/0377-8398(85)90007-6.

Winter, A., Henderiks, J., Beaufort, L., Rickaby, R.E.M., Brown, C.W., 2013. Poleward expansion of the coccolithophore Emiliania huxleyi. Journal of Plankton Research URL: `http://plankt.oxfordjournals.org/content/early/2013/11/27/plankt.fbt110.abstract`, doi:10.1093/plankt/fbt110, arXiv:`http://plankt.oxfordjournals.org/content/early/2013/11/27/plankt.fbt110.full.pdf+html`

Xu, J., Bach, L.T., Schulz, K.G., Zhao, W., Gao, K., Riebesell, U., 2016. The role of coccoliths in protecting *Emiliania huxleyi* against stressful light and UV radiation. Biogeosciences 13, 4637–4643. URL: `http://www.biogeosciences.net/13/4637/2016/`, doi:10.5194/bg-13-4637-2016.

Young, J.R., Brown, P.R., Lees, J.A., 2014. Nannotax3 website (URL: http://ina.tmsoc.org/nannotax3). URL: `http://ina.tmsoc.org/Nannotax3`.

Young, J.R., Geisen, M., Cros, L., Kleijne, A., Sprengel, C., Probert, I., Ostergaard, J., 2003. A guide to extant coccolithophore taxonomy. Journal of Nannoplankton Research, Special Issue 1 .

Ziveri, P., Thunell, R.C., Rio, D., 1995. Seasonal changes in coccolithophore densities in the Southern California Bight during 1991-1992. Deep Sea Research Part I: Oceanographic Research Papers 42, 1881–1903.

Zondervan, I., 2007. The effects of light, macronutrients, trace metals and CO_2 on the production of calcium carbonate and organic carbon in coccolithophores—a review. Deep Sea Research Part II: Topical Studies in Oceanography 54, 521 – 537. URL: `http://www.sciencedirect.com/science/article/pii/S0967064507000343`, doi:`http://dx.doi.org/10.1016/j.dsr2.2006.12.004`. the Role of Marine Organic Carbon and Calcite Fluxes in Driving Global Climate Change, Past and Future.

Zondervan, I., Rost, B., Riebesell, U., 2002. Effect of CO_2 concentration on the PIC/POC ratio in the coccolithophore Emiliania huxleyi grown under light-

limiting conditions and different daylengths. Journal of Experimental Marine Biology and Ecology 272, 55 – 70. URL: `http://www.sciencedirect.com/science/article/pii/S0022098102000370`, doi:`http://dx.doi.org/10.1016/S0022-0981(02)00037-0`.

1725

	POC-based μ		Cell-based μ	
	K_M (μatm)	μ_{max} (d^{-1})	K_M (μatm)	μ_{max} (d^{-1})
Median	51.0	0.99*	26.6	0.86*
Max	54.3*	1.6*	22.7*	1.4*
Min	40.2	0.45*	16.5	0.42*
Mean	**51.4***	0.99*	29.9*	0.93*

Table 1: Table of growth rate-specific pCO$_2$ half saturation constants and maximum growth rates in coccolithophores, derived from the compilation of data sources from listed in Table S1 (in the CO$_2$-μ column). Values are listed for both POC-based and cell-based growth rates (see section 4.1). The K_M value in bold was used in our coccolithophore model. Statistical significance of coefficients: *p<0.05.

Nutrient	Species	K_M	Reference
NO$_3$	*C. braarudii*	1.06 μM	Cermeño et al. (2011)
NO$_3$	*E. huxleyi* A	0.22 μM	Riegman et al. (2000)
NO$_3$	*E. huxleyi*	0.1 μM	Eppley et al. (1969)
NO$_3$	*E. huxleyi* A	0.35 μM	Perrin et al. (2016)
NO$_3$	*E. huxleyi* RCC911	0.14 μM	Perrin et al. (2016)
NO$_3$	*E. huxleyi* A	13.71 μM	Feng et al. (2016)
NH$_4$	*E. huxleyi*	0.15 μM	Eppley et al. (1969)
PO$_4$	*E. huxleyi* A	0.22 μM	Riegman et al. (2000)
PO$_4$	*E. huxleyi* A	0.051 μM	Perrin et al. (2016)
PO$_4$	*E. huxleyi* RCC911	0.31 μM	Perrin et al. (2016)
PO$_4$	*E. huxleyi* A	0.11 μM	Feng et al. (2016)
Fe	*E. huxleyi*	1.2 nM	Sunda and Huntsman (1995)

Table 2: Half saturation constants for nutrient uptake in coccolithophores. The mean K_M for PO$_4$ uptake, 0.17 μM, was used in our coccolithophore model. Note that the K_M for iron is in nM.
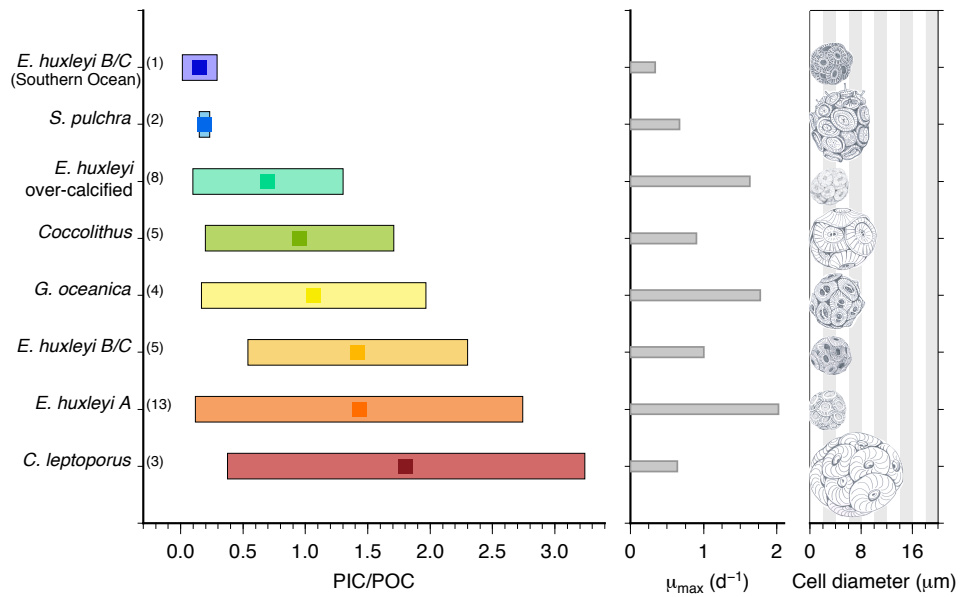
Figure 1: Ranges of published PIC/POC values, maximum growth rates (μ_{max}), and cell diameter of the eight coccolithophore subgroups used in this study. Coccolithophore subgroups are ordered based on midpoints (shown by brighter colored squares), with the lowest PIC/POC on top. Numbers in parentheses to the right of subgroup names represent the number of studies used to construct the PIC/POC ranges (all studies that have an 'x' in the any PIC/POC columns in Table S2 went into constructing these ranges).
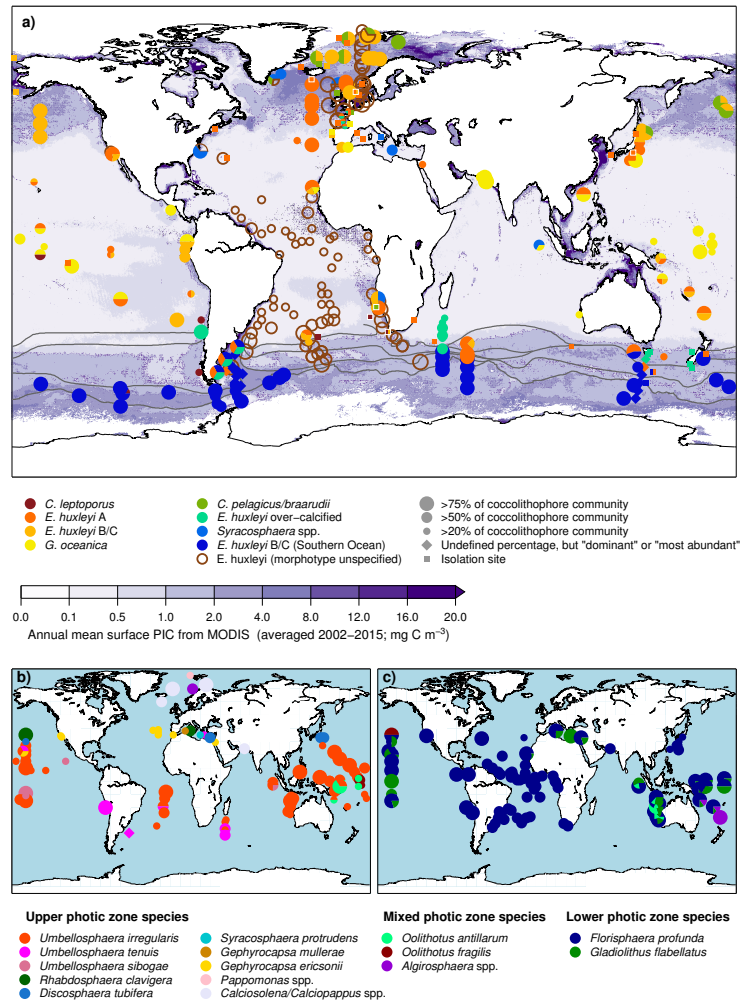
Figure 2: Geographical distributions of dominant (i.e., >20% of the coccolithophore population) coccolithophore subgroups. Panel (a) shows distributions of coccolithophore subgroups that have been cultured and physiologically studied in a laboratory, while the bottom two maps show lesser studied, uncultured coccolithophores from the upper photic zone (b) and the lower photic zone (c). The size of the dots refers to the relative abundance within the coccolithophore community at a particular location. MODIS satellite derived mean particulate inorganic carbon (PIC) concentration underlies the biogeographical data presented in map (a). PIC is a qualitative estimate of coccolithophore abundance. Antarctic circumpolar fronts are shown by gray lines; from the South pole to the equator the fronts are the Polar Front (Freeman and Lovenduski, 2016), the Subantarctic Front, South Subtropical Front, and North Subtropical Front (Belkin and Gordon, 1996).
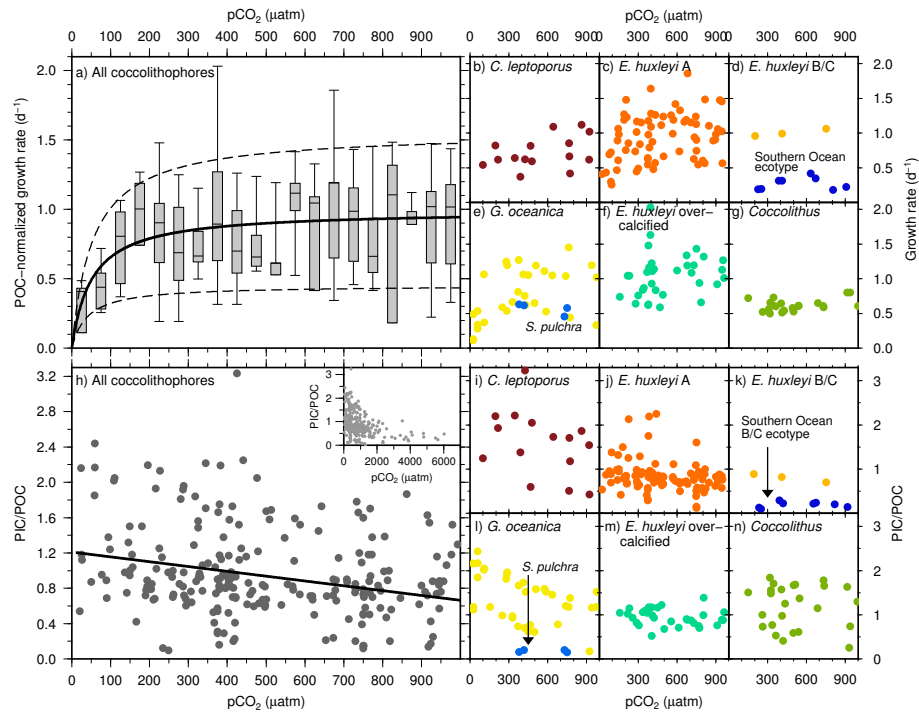
Figure 3: Published POC-based growth rates (see section 4.1) and PIC/POC ratios of all coccolithophore subgroups (a and h, respectively) and individual subgroups (b–g and i–n, respectively) as a function of pCO_2. Panel (a) shows minimum, quartiles, median and maximum growth rates within 50 μatm pCO_2 bins presented in a box-and-whisker plot. Michaelis-Menton curves in (a) were fit to the median (not shown), maximum and minimum quartiles (shown by dashed lines), and the mean (shown by black line). A least-squares line is shown in panel (h) for PIC/POC versus pCO_2 for pCO_2 values less than 1000 μatm. The small plot in the upper right corner of panel (h) shows the full range of the data compilation.
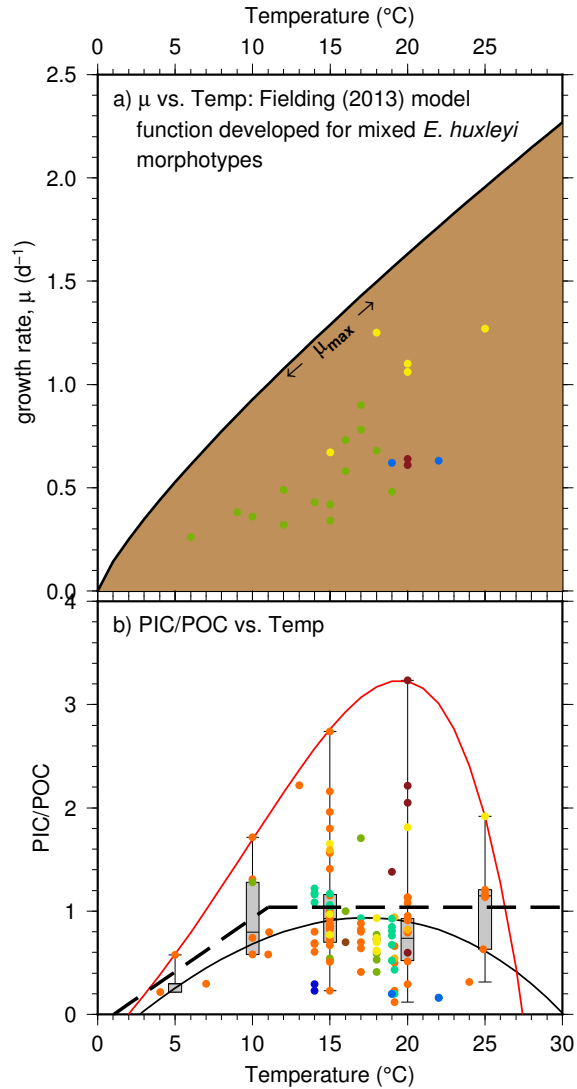
Figure 4: Growth rate (a) and PIC/POC (b) of coccolithophores as a function of temperature. In panel (a) a power function for predicting maximum growth rate (μ_{max}) from Fielding (2013) is shown for *E. huxleyi*. Other coccolithophore species growth rates are overlaid to demonstrate that this function encompasses all coccolithophore species. Panel (b) shows data from studies that measured PIC/POC ratios as a function of culturing temperature. Since PIC/POC can be influenced by CO_2 concentration or nutrient status, PIC/POC ratios shown in this figure are only from cultures grown at ambient CO_2 concentrations ($\sim$350 to 400 μatm) under nutrient replete conditions. Most PIC/POC measurements were made for cultures grown at stock culture temperatures, 15° to 20°. Colors of the dots correspond to the coccolithophore subgroups in Figure 2. The black line shows the PIC/POC-temperature function reported for *E. huxelyi* A by Feng et al. (2016), while the red line is this same function fit to the maximum binned data (5°C bins), shown by box-and-whisker symbols. The dashed black line represents the linear function used in our coccolithophore model, fit to data points for temperatures <11°C.
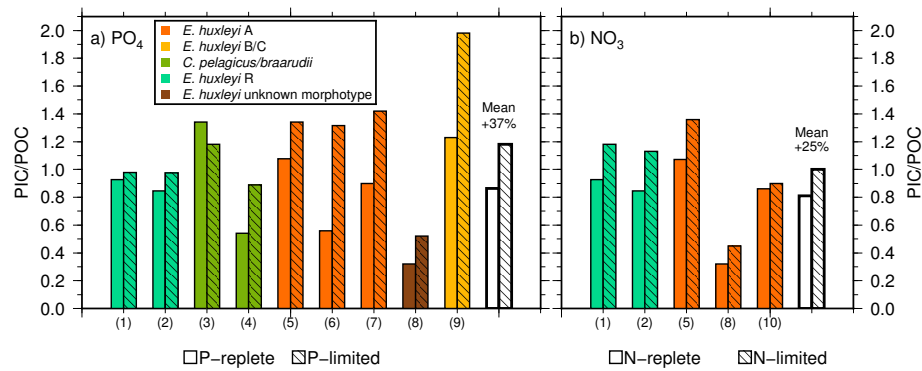
Figure 5: Published PIC/POC ratios of coccolithophore species or *E. huxleyi* morphotypes as a function of PO_4 (a) and NO_3 (b) limitation. All experiments were done at ambient CO_2 levels except for those from Rouco et al. (2013), which were done at 260 and 560 μatm for experiments 1 and 2, respectively. Numbers along x-axis correspond to references and experiments: 1. Rouco et al. (2013) at 260 μatm; 2. Rouco et al. (2013) at 560 μatm; 3. *C. braarudii* from Gerecht et al. (2014); 4. *C. pelagicus* from Gerecht et al. (2014); 5. *E. huxleyi* A from Paasche (1998); 6. *E. huxleyi* A from van Bleijswijk et al. (1994); 7. *E. huxleyi* A from Paasche and Brubak (1994); 8. *E. huxleyi* A from Perrin et al. (2016); 9. *E. huxleyi* B from van Bleijswijk et al. (1994); 10. *E. huxleyi* A from Feng et al. (2016).

68
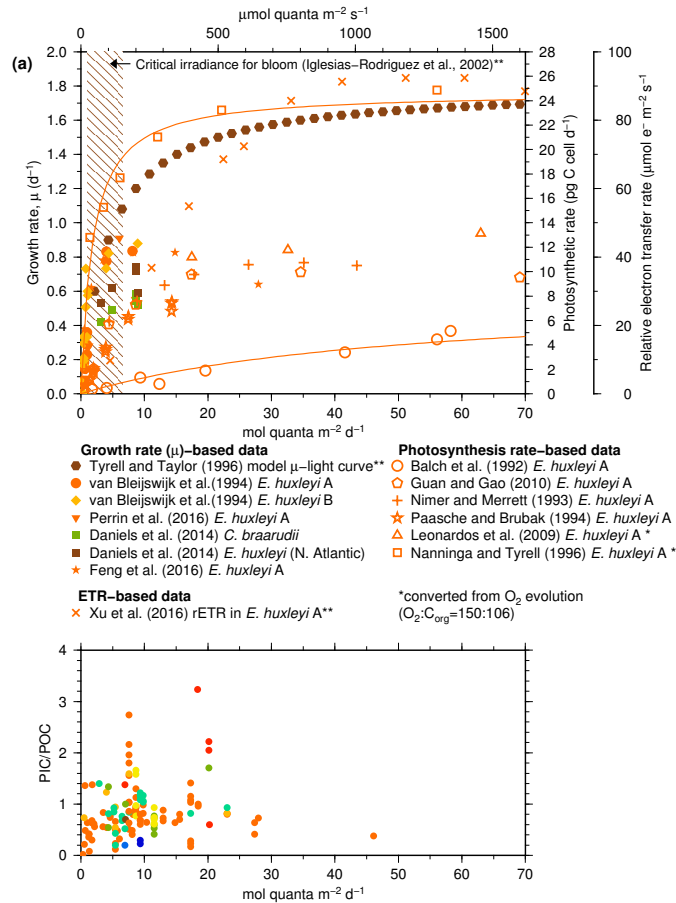
Figure 6: Growth rate, photosynthetic rate, or relative electron transfer rate (rETR) measured in coccolithophores as a function of irradiance from various studies (a) and PIC/POC as a function of irradiance (b). Colors in both plots correspond to coccolithophore subgroups specific in previous figures, while shapes in (a) correspond to specific references listed in the legend below. The Balch et al. (1992) data in (a) comes from the culture with 2 μM NO_3 added. The Nanninga and Tyrrell (1996) data in (a) refers to the culture of calcifying *E. huxelyi* (morphotype A) grown in Eppley medium. Culture pCO_2 levels range from 258 to 515 μatm and temperature ranges from 14°C to 20°C. Lines drawn on (a) represent Michaelis-Menten curve fits to the experiments showing the smallest (1.8 mol quanta m^{-2} d^{-1}; Nanninga and Tyrrell, 1996) and the largest (52.1 mol quanta m^{-2} d^{-1}; Balch et al., 1992) half saturation constants for light uptake. The hatched area refers to the critical irradiance for bloom formation from Iglesias-Rodríguez et al. (2002). All experiments were converted to irradiance units of mol quanta m^{-2} d^{-1}, except those marked with a double asterisk, which we were unable to convert and are reported in μmol quanta m^{-2} s^{-1} (top x-axis; Iglesias-Rodriguez et al., 2008; Tyrrell and Taylor, 1996; Xu et al., 2016). Top and bottom x-axes were aligned assuming a 12 hours of light per day.
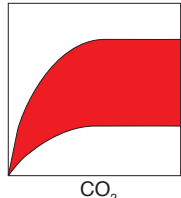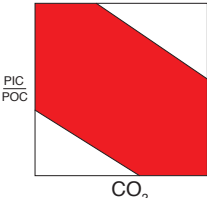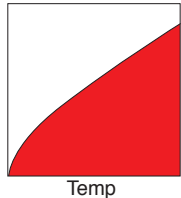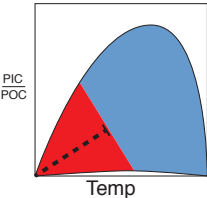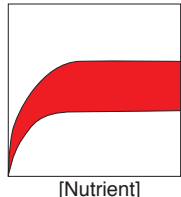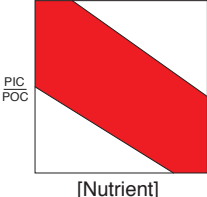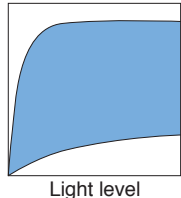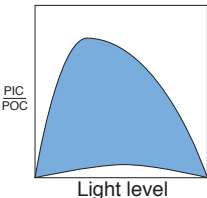
	Growth rate, μ (C_{org} production; d-1)		PIC/POC ratio	
pCO_2		• Carbon limited growth rate at low CO_2 • Large range of senstivities at high CO_2		• PIC/POC generally decreases as CO_2 increases • Large range of responses
Temperature		• Power function determines temperature dependent maximum growth rate		• PIC/POC decreases at low temperatures but the relationship at higher temperatures is not as clear
Nutrients		• Efficient nutrient uptake at low concentrations • Comparably high affinity for nutrients		• PIC/POC is higher under nutrient limitation and lower under nutrient replete conditions
Light		• Large range of irradiance curves • Some studies show fast growth at low light (bloom conditions)		• PIC/POC is lower at very low and high irradiance levels • Large PIC/POC range within typical irradiance

Figure 7: A graphical summary of relationships between coccolithophore growth rate and PIC/POC with changing pCO_2, temperature, nutrients and light. Relationships depicted in red are used in our global coccolithophore model.
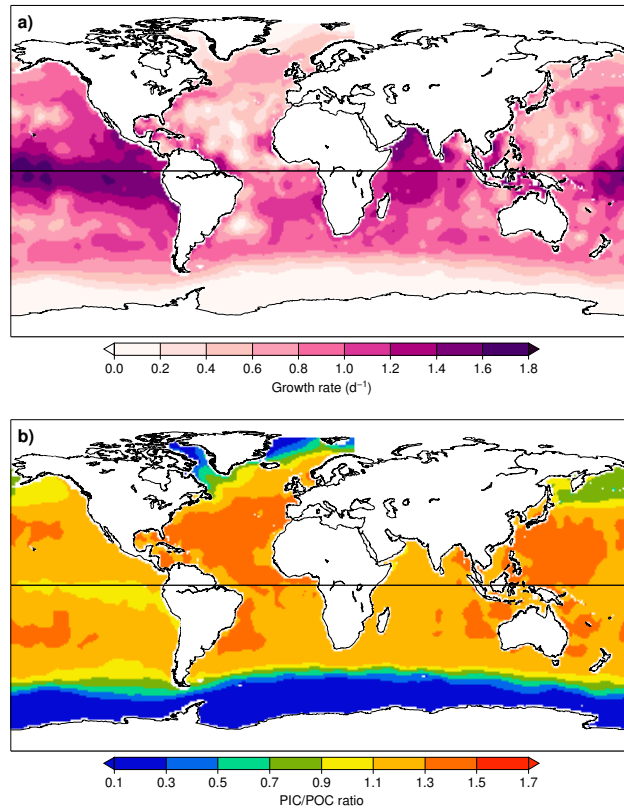
Figure 8: Present day surface coccolithophore growth rate (a) and PIC/POC ratio (b) during the growing season (June-July-August mean for Northern Hemisphere and December-January-February mean for Southern Hemisphere; division shown by black line at equator) derived from our coccolithophore model driven by monthly mean sea surface temperature and PO_4 concentration from GLODAP (Lauvset et al., 2016) and monthly mean pCO_2 from Landschützer et al. (2015).
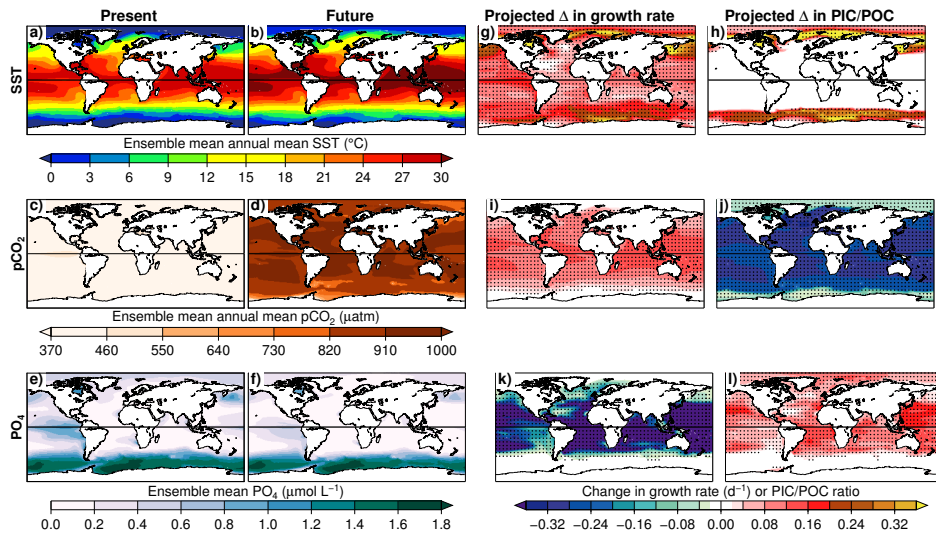
Figure 9: Ensemble mean output for decadal averages of growing season (JJA mean for Northern Hemisphere; DJF mean for Southern Hemisphere) sea surface temperature (SST), pCO_2, and PO_4 concentration for the present-day (2006–2015) and future (2091–2100) from the CESM-LE (maps (a)–(f)) and change maps from our global coccolithophore model showing the changes in coccolithophore growth rate and PIC/POC during the growing season resulting from each individual driver: sea surface temperature, (g) and (h); pCO_2, (i) and (j); and PO_4, (k) and (l). Stippled area shows significant changes (i.e., signal-to-noise ratio >2; see Methods).
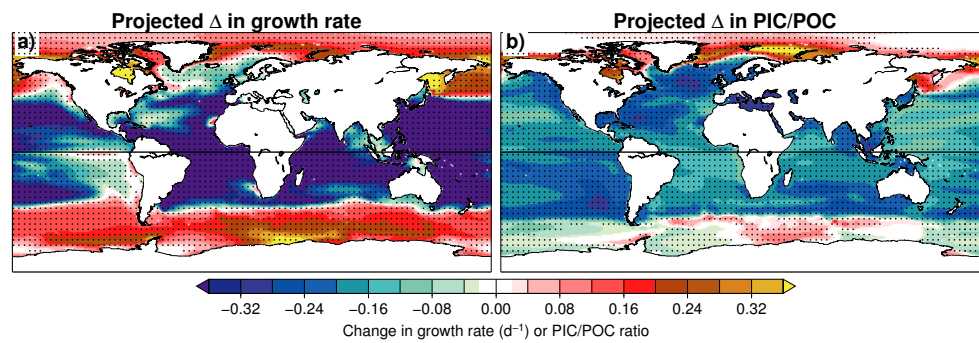
72

Figure 10: Changes in coccolithophore growth rate and PIC/POC during the growing season (JJA mean for Northern Hemisphere; DJF mean for Southern Hemisphere) from the combined effects of CESM-simulated 21st century changes in monthly mean sea surface temperature, pCO_2, and PO_4 from the start (2006–2015) to the end (2091–2100) of the 21st century. Maps depict the CESM-LE ensemble mean changes with significant changes shown by stippled area (i.e., signal-to-noise ratio >2; see Methods).